Muhammad Fuad Farooqi

A Master's Thesis

AGU 2022

DEVELOPMENT OF A PAPER BASED MAGNETOPHORETIC SENSOR

A THESIS
SUBMITTED TO THE DEPARTMENT OF ELECTRICAL AND COMPUTER ENGINEERING
AND THE GRADUATE SCHOOL OF ENGINEERING AND SCIENCE
OF ABDULLAH GUL UNIVERSITY
IN PARTIAL FULFILLMENT OF THE REQUIREMENTS
FOR THE DEGREE OF
MASTER OF SCIENCE

By
Muhammad Fuad Farooqi
January 2022

DEVELOPMENT OF A PAPER BASED MAGNETOPHORETIC SENSOR

A THESIS
SUBMITTED TO THE DEPARTMENT OF ELECTRICAL AND COMPUTER ENGINEERING
AND THE GRADUATE SCHOOL OF ENGINEERING AND SCIENCE OF ABDULLAH GUL UNIVERSITY
IN PARTIAL FULFILLMENT OF THE REQUIREMENTS
FOR THE DEGREE OF
MASTER OF SCIENCE

By
Muhammad Fuad Farooqi
January 2022

SCIENTIFIC ETHICS COMPLIANCE

I hereby declare that all information in this document has been obtained in accordance with academic rules and ethical conduct. I also declare that, as required by these rules and conduct, I have fully cited and referenced all materials and results that are not original to this work.

Name-Surname: Muhammad Fuad Farooqi
Signature :

REGULATORY COMPLIANCE

M.Sc. thesis titled Development of a Paper-based Magnetophoretic Sensor has been prepared in accordance with the Thesis Writing Guidelines of the Abdullah Gül University, Graduate School of Engineering & Science.

Prepared By	Advisor
Muhammad Fuad Farooqi	Assoc. Prof. Kutay İçöz

Head of the Electrical and Computer Engineering Program

Assoc. Prof. Kutay İçöz

ACCEPTANCE AND APPROVAL

M.Sc. thesis titled Development of a Paper-based Magnetophoretic Sensor and prepared by Muhammad Fuad Farooqi has been accepted by the jury in the Electrical and Computer Engineering Graduate Program at Abdullah Gül University, Graduate School of Engineering & Science.

21/01/2022

(Thesis Defense Exam Date)

JURY:

Advisor : Assoc. Prof. Kutay İçöz

Member : Asst. Prof. Talha Erdem

Member : Asst. Prof. Ömer Aydın

APPROVAL:

The acceptance of this M.Sc. thesis has been approved by the decision of the Abdullah Gül University, Graduate School of Engineering & Science, Executive Board dated ….. /….. / …….. and numbered ……..……. .

…….. /…….. / ……..

(Date)

Graduate School Dean
Prof. Dr. İrfan Alan

ABSTRACT

DEVELOPMENT OF A PAPER BASED MAGNETOPHORETIC SENSOR

Muhammad Fuad Farooqi
MSc. in Electrical and Computer Engineering
Advisor: Assoc. Prof. Kutay İçöz

January 2022

One of the widely used type of biosensors are paper-based lateral flow systems. They are used to detect a wide variety of biomolecules like microorganisms, proteins, chemicals, oligonucleotides among many others. In this research, a setup was created using dual magnet sets in which the flow of cell sample on two kinds of different sample paper was explored. There were two factors which affected the movement of the sample the most, the magnetic field and the wetting. Images were obtained using a cell phone along and/or a bright field optical microscope and then analyzed using image processing. Images were also taken using scanning electron microscope. The effects of the wetting and the magnetic field were tested and studied. It was found that at least 90% of the cells were able to reach the edge of the paper. Although the cells were not able to maintain their shape on the paper due to the unideal conditions of the paper for cells but still this kind of paper-based lateral flow assay setup can be used for cells to see their behavior when they were labelled and exposed to a magnetic field. This research shows support that this technique can be used for separating cells as well as detecting different cells.

Keywords: Paper-based biosensor, cell separation, magnetic force, fluid-flow, immunomagnetic particles

ÖZET

KAĞIT TABANLI MAGNETOFORETİK SENSÖR GELİŞTİRİLMESİ

Muhammad Fuad Farooqi
Elektrik ve Bilgisayar Mühendisliği Anabilim Dalı Yüksek Lisans
Tez Yöneticisi: Doç. Dr. Kutay İçöz

Ocak 2022

Yaygın olarak kullanılan biyosensör tiplerinden biri kağıt tabanlı yanal akış sistemleridir. Bu sistemler mikroorganizmalar, proteinler, kimyasallar, oligonükleotitler ve diğerleri gibi çok çeşitli biyomolekülleri tespit etmek için kullanılırlar. Bu araştırmada, hücre numunesinin akışının iki çeşit farklı numune kağıdı üzerinde araştırıldığı ikili mıknatıs setleri kullanılarak bir düzenek oluşturulmuştur. Numunenin hareketini en çok etkileyen iki faktör manyetik alan ve ıslanmadır. Bu çalışmada ki görüntüler bir cep telefonu ve/veya parlak alan optik mikroskobu kullanılarak elde edilmiş ve ardından görüntü işleme kullanılarak analiz edilmiştir. Ayrıca bazı örnekler taramalı elektron mikroskobu kullanılarak görüntülenmiştir. Bu çalışmada ıslanmanın ve manyetik alanın etkileri test edilmiş ve incelenmiştir. Hücrelerin en az %90'ının kağıdın kenarına ulaşabildiği gözlenmiştir. Kağıdın hücreler için ideal olmayan koşulları nedeniyle hücreler kağıt üzerinde şekillerini uzun süre koruyamasa da, bu tür kağıt tabanlı yanal akış sistemleri önemli avantajları nedeniyle, hücresel uyuglamlar için potansiyel barındırmaktadır ve hücreleri algılamak için kullanılabilir. Bu çalışma, manyetik alanın ve kağıt temelli platformların hücreleri ayırmak ve farklı hücreleri tespit etmek için kullanılabileceğini göstermektedir.

Anahtar kelimeler: Kağıt bazlı biyosensör, hücre ayırma, manyetik kuvvet, sıvı akışı, immünomanyetik parçacıklar

Acknowledgements

I would like to express my deepest gratitude to my academic advisor and head of department Associate Professor Kutay İçöz, who supported me throughout my years at Abdullah Gul University. I was lucky to be able to work under him as I got the chance to improve myself by learning from him, from his experiences and from his never-ending guidance. He provided me with constant support and trust, pushing me and motivating me to work hard and became a bridge that led me to get to where I am academically and in life.

Assistant professor Şerife Ayaz Güner, had guided me with her knowledge and had taken out the time to help me and for that I would like to extend my sincere gratitude.

My best friend, Halid Alabay, has gone above and beyond for me, always being there to help me even though he had been busy with his work. He did not only provide help for my work but also provided emotional support that I needed being away from my home and loved ones.

I would also like to thank my fellow master's student Dudu Boyvat for helping me with cell cultures and my expeirments. She has been a great support in my research.

In my work, there were times when I needed help with getting certain materials or understanding a concept or even a procedure that I couldn't understand and I was lucky to be with students, teaching assistants and research assistants of AGU who were always helping with a smile, to name a few, Merve Şansaçar, Osman Oğuz, Zeynep Şenel, Ruby Phul, Helin Sağır and Fatma Betül Köşker.

Adam Thahir, my first friend in Turkey and my housemate, is one person who I was always asking for help whenever I would get stuck with programming. His skills in programming have always been inspirational to me.

My parents, Muhammad Asad Farooqi and Shamaila Asad who were always there to share their vast experience and knowledge about engineering and research. They always had a suggestion for me to improve my work, research, write-up and even presentations.

My older sister and my older brother Fareeha Usman and Hammad Farooqi have always been my biggest supports and care-takers after my parents.

Sayed Zakee Irfan Qadri has been like a brother to me and has provided me with support and time whenever it would get stressful and challenging.

TABLE OF CONTENTS

LIST OF FIGURES

LIST OF TABLES

LIST OF ABBREVIATIONS

LOC	Lab on Chip
LFB	Lateral flow biosensor
IMB	Immunomagnetic beads
PBS	Phosphate-buffered saline
BSA	Bovine serum albumin

To my parents
Muhammad Asad Farooqi
and
Dr. Shamaila Asad
For Their Never-ending Support and Love

Chapter 1

Introduction

1.1 Biosensors

Biosensors are common for biomedical diagnosis, and they also have a wide variety of applications such as detection and treatment of a disease, testing food for contaminants, testing for drugs, forensics and research based on the field of biomedical engineering. Many different methods can be used to create biosensors [1]. Glucometer is an example of an everyday biosensor, it uses the enzyme glucose oxidase as an electrode, using electrochemical detection of oxygen or hydrogen peroxide to detect glucose. Biosensors is a wide topic and can involve the use of many different strategies and techniques for sensing purposes. Following are some types of biosensors:

- Electrochemical Biosensors
- Optical/Visual Biosensors
- Silica, Quartz/Crystal and Glass Biosensors
- Nanomaterials-Based Biosensors
- Genetically Encoded or Synthetic Fluorescent Biosensors
- Bio micro-electro-mechanical Biosensors [2-4]
- Microbial Biosensors [5]

Biosensors are made not only with the aim to create a specific, quick, and accurate device but sometimes the aim is to make a cheap device that can be used for medical purposes to be used places that do not have proper access to medical facilities and labs [6]. Point of Care (POC) testing is a decentralized approach to diagnostic analysis, this can be performed in the patient's room, in their hospital bed, operation theater, clinics or in remote areas that do not have access to facilities. The idea is to decrease the size of the instrument and the procedures involved [7]. In the research by Ung et al., a POC device called the "HemeChip" was created to detect sickle cell disease using a cellphone. The chip was using a cellulose acetate based electrophoresis to quickly separate the different

types of hemoglobin in the blood, while requiring less than 5 µl of blood sample, which can be easily obtained [6].

Biosensors can be used to detect a wide variety of diseases. Cells were separated using immunomagnetic separation where nano and micro size beads were used to separate blast cells (cancer cells) [8,9]. Similarly CD19 antibodies were used with different kinds of surface functionalization to see their effect in capturing of B lymphoblast cells associated with acute lymphoblastic leukemia disease [10]. A microfluidic chip biosensor was developed which was able to monitor the amount of blast cells in the bone marrow samples of leukemia patient, to track the effectiveness of chemotherapy that they were receiving for acute lymphoblastic leukemia [11].

1.2 Magnetophoresis

Magnetophoresis is a process that involves the separation of particles using magnetic forces. In biomedical sensors this process is used to separate different kinds of biological materials at the nano or micro level. There are two types of magnetophoresis, positive and negative magnetophoresis. In positive magnetophoresis, magnetic particles are moved through a diamagnetic medium while in negative magnetophoresis, diamagnetic particles are moved in a magnetic medium. In order to perform Magnetophoresis a gradient in the magnetic field, a gradient in the magnetization of the medium itself, or it could be a conjunction of both [12].

Magnetophoresis has different applications, in the research done by Huang et al. Circulating Tumor Cells were separated using a specialized magnetophoretic microchannel which had specialized structures to increase the effect of magnetic force (Figure 1.1) [13]. In the research by Osman et al. immunomagnetic cells were separated using a microfluidic channel with patterned magnetization which lead to a high amount of trapping of cells [14]. Darabi and Guo developed a microfluidic chip which was performing magnetophoresis to obtain only monocytes from human blood. The chip was using a negative selection method where all the other cells were trapped inside the chip while only the monocytes were only let to flow out of the chip [15]. Xia et al. created a microfluidic magnetophoretic device that could perform continuous separation of living cells. Laminar flow and magnetic separation were implemented for this experiment where a high magnetic force was creating by a magnetic field gradient which was achieved using

a special microfabricated comb like structure [16]. Magnetophoresis can also be used for separating bacteria as done in the research by Pivetal et al. a pattern with magnetized and reverse magnetized regions was created on a surface of a silicon wafer. The pattern with the reversed magnetizations led to regions of high magnetic field gradient which resulted in high magnetic force being applied on the particles [17].

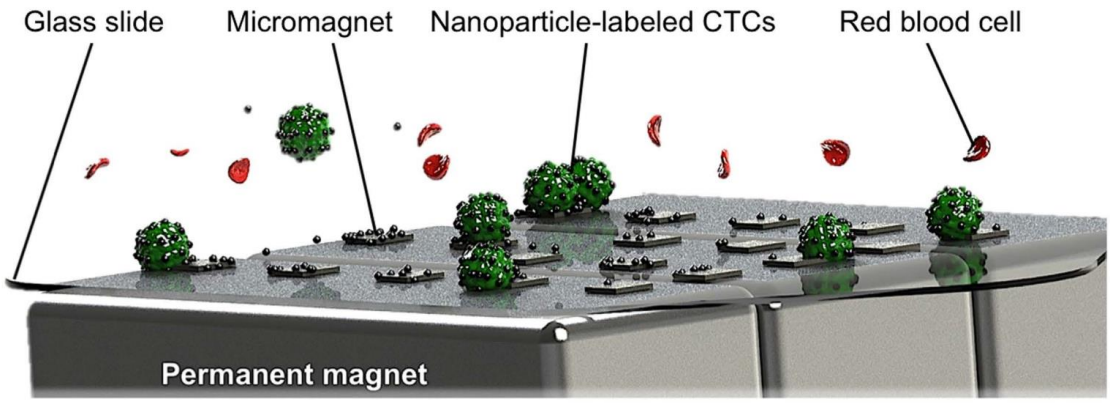

Figure 1.1 Magnetophoretic channel with specialized magnetic structures[13].

1.3 Lateral Flow Biosensors

Lateral flow biosensors (LFBs) are a kind of biosensors that are paper based. They are an advanced version of the paper immunoassays. They show the most important characteristics of an ideal biosensor, high sensitivity, low limit of detection and good selectivity. Moreover, being low cost, and time efficient and robust systems which are desired qualities. They have their drawbacks or weaknesses as well, often the response obtained from them is through the naked eye which would give qualitative results and not quantitative results. This drawback could be overcome by using reading devices i.e., taking images and processing them, the other drawback is that the sample needs to be viscous in order to be able to flow through the paper. Since the medium is paper the pores could be blocked hindering the flow of the material, this could result in unspecific adsorption giving wrong results [18]. In Figure 1.2 the typical structure of an LFB is shown. The LFB has a sample pad where the sample is added, the sample pad also confirms the characteristics of the sample to match those required for ideal detection. After that, the sample meets the conjugate pad. The conjugate pad has labeled detection bioreceptors which are released, the wetting causes the first analyte-bioreceptor interaction. The sample then continues through the membrane. Generally, the LFBs have two lines present on the membrane, the test line which confirms that the labeled analyte

is travelling through the sample paper. The second line is the control line. This confirms that the LFB is working. The first line gives the results while the second is a control check. At the end the absorbent pad is present, the purpose of the absorbent is to provide enough bed volume to cause the proper flow of the sample the structure of this is shown in Figure 1.2 [19]. LFBs have applications for use of detecting hazardous materials, heavy metals, allergens and pathogens in food, pesticides, drugs [20–26]. The performance of lateral flow assay was improved by the use of electromagnetism. The reporter particles were relocated by using electromagnetism. They were able to design a device which had an increased sensitivity of human chorionic gonadotropin detection, and also an increased color intensity per particle was observed on the strip[27].

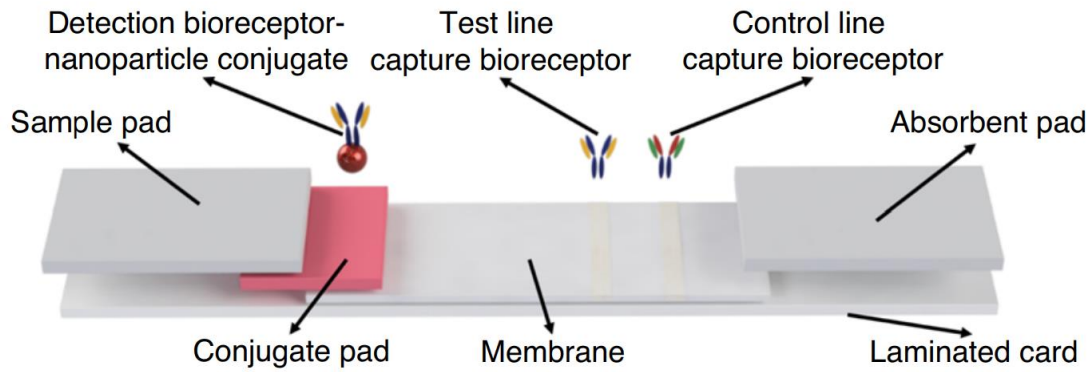

Figure 1.2 The general structure of a typical LFB[19].

1.4 Micro/Nano Magnetic Particles

For magnetophoretic applications micro sized or nano sized magnetic particles are used. These particles are usually superparamagnetic particles, one of the commonly used superparamagnetic particle is iron oxide based, like maghemite. [28] The other kind of particles are ferromagnetic particles. For ferromagnetic particles even after a previously applied magnetic field is removed, they have net magnetic dipole moments, as for the paramagnetic particles they have aligned dipoles only when there is an external magnetic field applied. Figure 1.3 shows the magnetic behavior of different kinds of magnetic materials under an applied field. The type of magnetic behavior is important in magnetophoresis because it affects the way the particles interact. If the particles are ferromagnetic, they clump up to each other which is unideal. Superparamagnetic particles on the other hand don’t clump-up together and thus only experience the magnetic force this makes them ideal for magnetophoresis [29]. Magnetic particles are also used for

sensitivity enhancement [30] and signal amplification [31,32]. For signal amplification, the magnetized magnetic particles act like a magnet and attract other magnetic particles nearby.

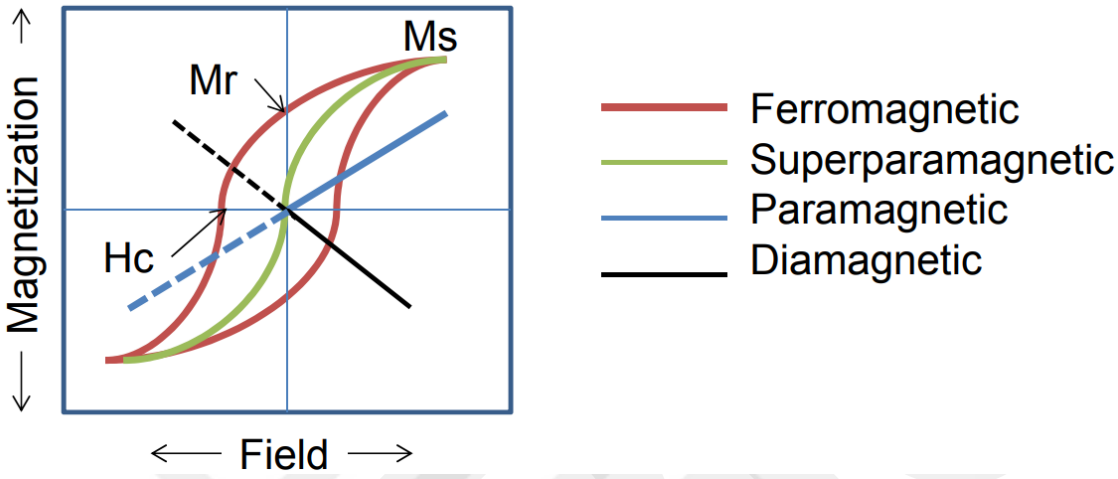

Figure 1.3 Magnetic behavior of different types of magnetic material under a magnetic field [29].

Immunomagnetic beads (IMB) are a kind of magnetic particles which have surfaces functionalized by specific antibodies. These antibodies are used to bind to specific proteins or molecules which might be present on the membrane of a cell. Immunomagnetic beads are highly specific and thus cannot be used for labeling a wide type of cells [33]. Thus, specific cells can be labelled and separated using this kind of approach. Immunomagnetic beads with a specific antibody can be used to label cells expressing a specific antigen or surface protein as done in the research by İçöz et al. [9]. Figure 1.4 shows an SEM image of Invitrogen CD45 Dynabeads on MilliporeSigma Hi-Flow™ Plus HF075.

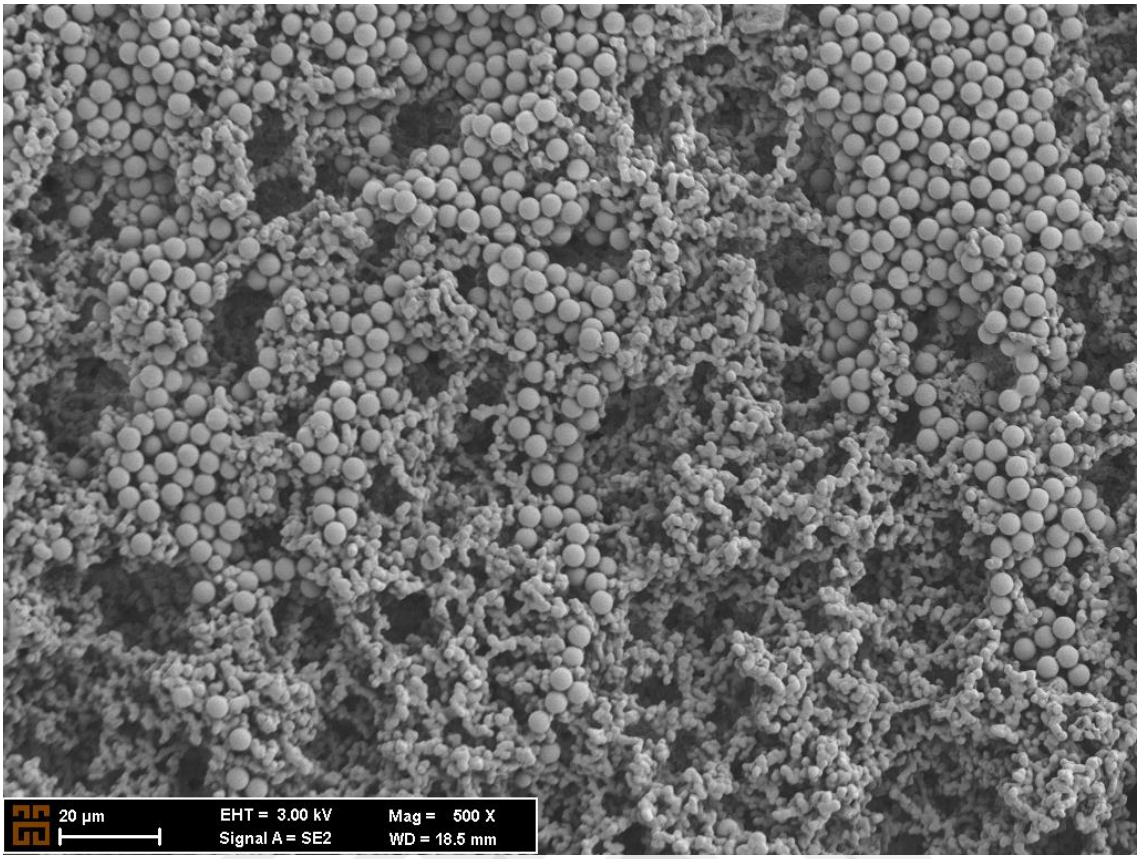

Figure 1.4 Immunomagnetic beads on sample paper.

1.5 Antibodies

As mentioned earlier IMBs have antibodies on them which allow them to bind to different kinds of biological materials i.e., antigens. They are useful in biosensors because they can be specific and at the same time, they allow us to bind magnetic beads to them. Antibodies are made up of proteins and they are created by B white blood cells. Generally, antibodies help aid the body fight pathogens. Antibodies interact with the antigens on top of the pathogens causing them to be destroyed. The body's immune system can make up to millions of different kinds of antibodies, which can attach themselves to any type of substance that the body can come into contact with. Antibodies are specific though and can only interact with one or a few similar antigens. Antibodies are considered globular protein and they are composed of two kinds of polypeptide chains, heavy chains which are larger and light chains which are smaller. These two chains are connected to each other by disulfide bonds. Antibodies are also known as immunoglobulins and there are five types: IgA, IgD, IgE, IgG and IgM [34].

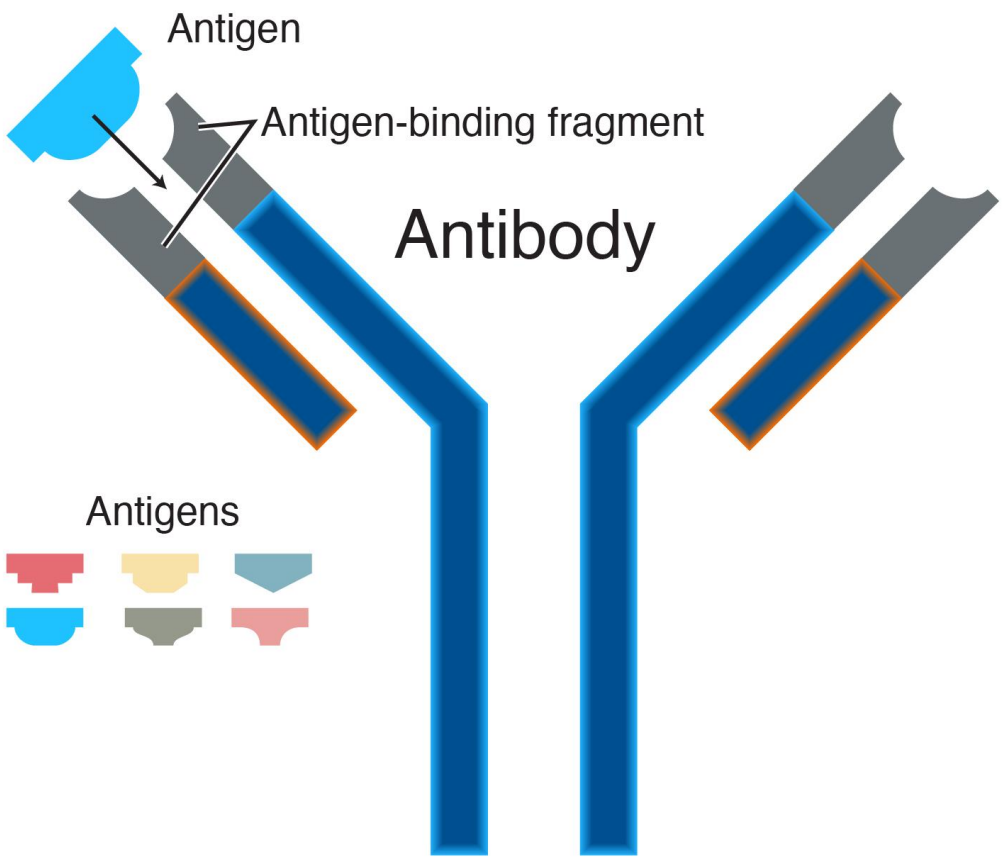

Figure 1.5 Structure of an antibody[35]. Antibodies are Y-shaped and have a antigen-binding fragment from where it binds to antigens.

The antigen-binding fragment of the antibodies vary amongst each other. This allows them to attach to a specific antigen. The antibodies have complementary structures to the antigens, forming bonds among them. The cell surface has different kinds of antigens and these can differ from cell to cell (Figure 1.5) [34]. Immunomagnetic beads are functionalized with antibodies on their surfaces[9].

1.5 Forces

In a microfluidic system the force balance on a moving particle can be shown by equation 1.

$$m_p \frac{du_p}{dt} = F_m + F_g + F_d + F_B + F_L \quad (1)$$

Where the mass of the particle is given by m_p, u_p is the velocity of the particle. F_m, F_g, F_d, F_b and F_L are magnetic force, gravity force, drag force, Brownian force and lift force,

respectively. For micron sized particles the most dominant force is the magnetic force [36]. The magnetic force on the particle can be represented by equation 2.

$$F_m = \frac{V_p \Delta\chi}{2\mu_0} (\boldsymbol{B}.\nabla)\boldsymbol{B} \qquad (2)$$

V_p is the volume of the particle, $\Delta\chi$ is the difference between the magnetic susceptibilities of the material of the particle and the medium the particle is in. B is the magnetic field, μ_0 is the magnetic permeability [37]. In the research [38], they were able to produce about 25 pN magnetic force on the particles which were micro sized particles while the electromagnetics in the research had generated 50 – 100 mT magnetic field.

1.6 Fluid Flow on Paper

The fluid flow in paper takes place due to the capillary action and this can be modelled through different approaches. The classical model, Lucas-Washburn equation is used to explain the flow of the fluid in a porous media. The model assumes that media is made up multiple capillary tubes which are set up parallel to each other and have the same diameter[39].

$$L^2 = \frac{\gamma \cos(\theta) r}{2\mu} t \rightarrow L^2 = kt \qquad (3)$$

Equation 3 is the Lucas-Washburn equation. L is the distance travelled by the fluid because of the capillary pressure and is a function of the wicking time (t). γ is the surface tension, θ is the liquid contact angle, r is the pore radius, μ is the fluid viscosity and k is the constant which represents the slope of the graph of L^2 and t, it can also be called diffusivity [40].

The cells were first fixed and then labelled by antibody conjugated IMBs. To make the cells visible on the paper, the cells were then stained using Trypan blue dye. Then after the sample was added to the midpoint of the pre-wetted sample paper, a parallel magnetic field was then applied, which made the sample move to the edges of the paper due to the magnetic field that was created between the poles of the two magnet sets. Then images were taken by using a mobile phone or a bright field optical microscope (Figure 1.4a). These images were then processed using a python code (Figure 1.4b). This research

explores the effect of magnetic field and wetting on the separation and the accumulation of the magnetic particles and cells.

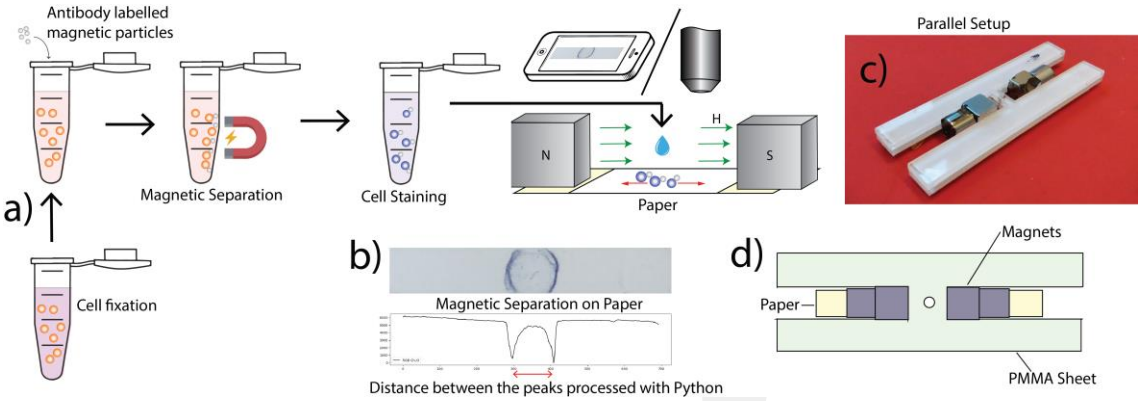

Figure 1.6 The outline of the experiment.

Chapter 2

Materials and Methods

2.1 Magnetic Platform

The magnetic platform was created using 4 Neodymium magnets. 2 cube shaped magnets of dimensions 1.2 cm x 1.2 cm x 1.2 cm and 2 cylinder magnets of dimensions of 1.2 cm x 1.2 cm. The idea was to create a concentrated magnetic field between two magnets. To achieve this the magnets needed to be separated and it needed to be made sure that the magnets would not touch each other. To create such a platform two acrylic sheets of 3.175 mm thickness were used. Two H shaped pieces were designed using CoralDRAW and cut using the laser cutter. The two pieces were stuck together using double sided tape. Two pieces were used to increase structural integrity. In the middle of the H shaped pieces there was a hole to the add the sample from, but it was not used since it was magnetizing the sample before it was added on to the paper.

The magnets were placed into the acrylic sheet sandwich as shown in Figure 2.1. This platform was used throughout the research for the other experiments because it allowed the change of the magnetic field by varrying the distance between the two magnet sets. The platform held the magnets very well and the distance between the magnets did not change even when the platform was left for days. For the experiments done with the platform only one side of the magnet platform was always let facing top and the direction was also always kept the same for standardization purposes.

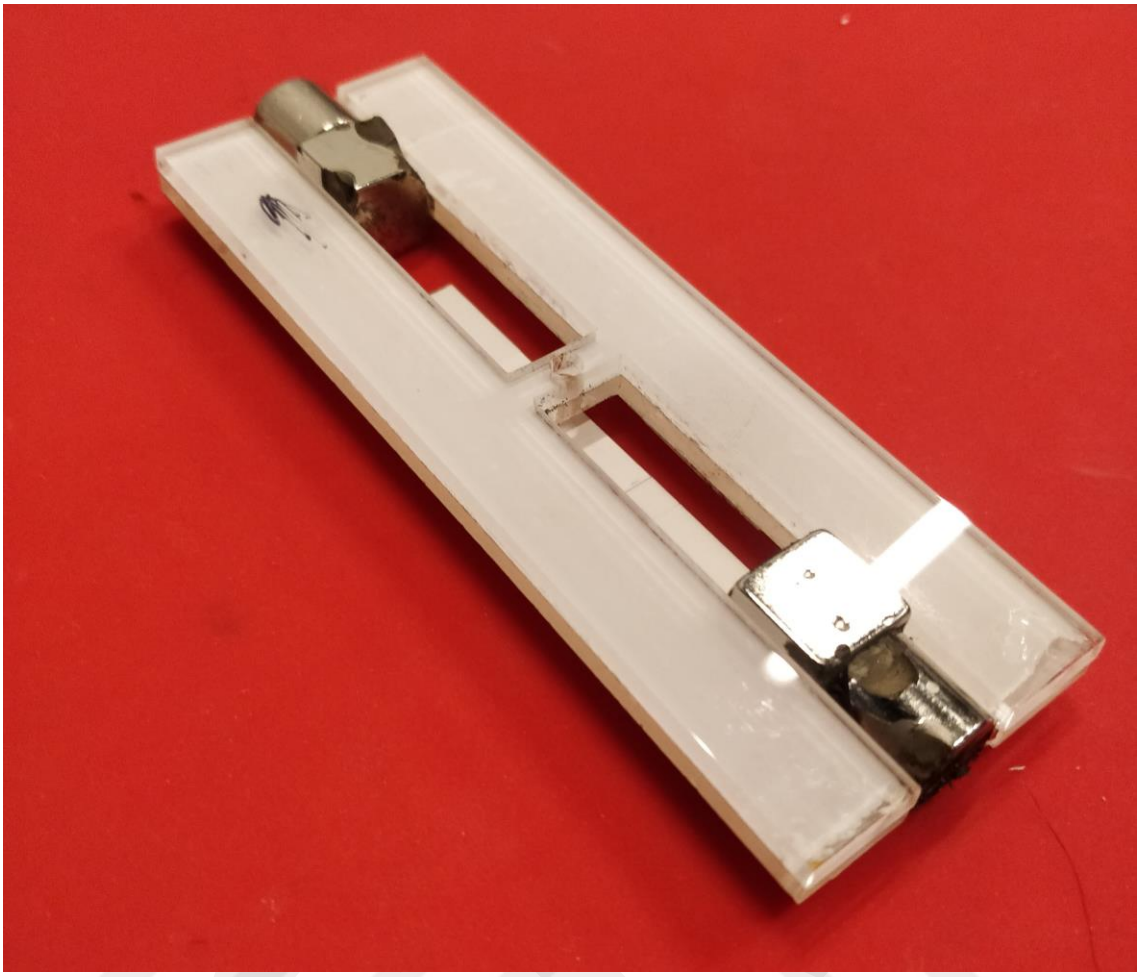

Figure 2.1 The magnetic platform, there were two sets of Neodymium magnets and the PMMA sheets were holding them apart making a strong magnetic field in the middle.

2.2 Magnetic Force

Magnetic force can be applied using either electromagnets [38, 41, 42] or permanent magnets [31, 32]. In this study the magnetic force was applied using two magnets that were coupled on a contraption to keep them facing towards each other without making contact so the magnetic field could be concentrated in the middle. Dynabeads CD45 were used for this experiment. The solution was made of 26.7 million particles/ml. The distance between the two magnets was increased which caused the decrease in the magnetic field. The distance was varied from 2.5 cm which led to 87.7 mT to 8.0 cm which lead to 8.3 mT. The paper was first wetted using deionized water and then the sample was added right in the middle of the paper after which the magnetic field was applied on the paper causing the particles to move and separate on the paper. The paper was left in the magnetic field for 10 minutes after which the magnetic field was

removed. The images of the paper were then taken using a cellphone and processed using the Python code. The magnetic force was measured using a gauss meter. The FWBELL Model 1500 was used.

2.3 Wetting

In the experiments on paper wetting is an important factor which affects the separation and the movement of particles on the paper. For these experiments, the paper was wetted with different amounts of PBS. The PBS amount was changed from 10 µl to 30 µl. For this experiment the paper was wetted for 10 minutes after which the sample with just Dynabeads with CD45 was added. 5 µl of the sample was added after which the magnetic field was applied, and the paper was left for 10 minutes. For values of 10, 15 and 20 µl the distance between the magnets was kept to 1.5 cm (276.7mT). For 25 and 30 µl the distance was kept to 2.75 µl (117.5 mT) The images were taken and then processed using the Python code.

2.4 Paper-Based Magnetophoresis

For this experiment Millipore Hi-Flow Plus HF135 and Millipore Hi-Flow PlusHF075 were used. Leukemia cells of the cell line K562 were used.

2.4.1 Cell Preparation

The cells used for this experiment were K562 Leukemia cells. The cells were obtained from the Molecular Biology and Genetics Department of Abdullah Gul University. The cells were initially thawed and put in 10% FBS RPMI cell medium. The cells were passaged depending on their numbers but usually a passage was done every two days. For the passage, the cells were taken from their flasks or trays and then they were centrifuged at 500 G for 5 minutes. After which the supernatant was thrown and fresh 10% FBS RPMI solution was added. The cells were then centrifuged again, and the last step was repeated. The cells were suspended in a 5 ml medium solution after which 10 µl of the cell solution and a 10 µl of trypan blue were mixed and a cell counting chamber was used to count the number of cells under the microscope. According to the number of cells, the solution was divided into different containers and more cell medium was added. The cells were kept in an Incubator with the temperature set to 37.0 °C with the CO_2 concentration of 5%. All of the work done with the cells was done inside a

laminar flow hood to avoid contamination. The hood was sterilized with alcohol before use. All the equipment that was put inside the laminar flow was first doused in alcohol to sterilize it. After using the laminar flow hood the hood was sterilize, using UV light. Special care was taken towards sterilization since the cells could easily be affected by contaminations. The prepared medium used for the cells was also first warmed up to 37 °C.

The cells were first centrifuged at 400 G for 5 minutes and washed to remove the cell medium. The cells were then counted, and they were then fixed. The cell fixing was done using paraformaldehyde, Paraformaldehyde was added according to the number of cells. For 3 million cells, 3 ml of 4% Paraformaldehyde solution was added along with 3 ml of PBS. After making this solution with the cells, the solution was put into a 15 ml Falcon tube and then put onto a rotator for 15 minutes. After the rotator, the sample was centrifuged at 400 G for 5 mins. The process was repeated 3 times washing with PBS every time. MACS buffer was prepared using, 10 mg of BSA and 20 µl of EDTA topped up to 20 ml of a solution using PBS. Invitrogen Dynabeads CD45 were washed with the MACS buffer using the magnetic rack showed in the Figure 2.3. The magnetic rack would apply a magnetic field on the solution attracting the magnetic particles in the solution and making them accumulate on the wall after which the rest of the liquid from the Eppendorf tube can be replaced. 20 µl of Dynabeads were washed in the Eppendorf tube. The cell sample was suspended in the MACS buffer after which it was added to the washed Dynabeads. The sample was then again put onto the rotator for 15 mins at 4°C. After the rotator, the sample was washed with PBS using the magnetic rack 3 times. The sample was then stained using Trypan Blue. The cells were added to a 500 µl PBS and 500 µl of a 0.5% trypan blue solution. The solution was gently mixed and left for 5 minutes. After five minutes the magnetic rack was used to separate the cells and the sample was washed using PBS, 3 times. In the end this led to a cell sample which was stained and labelled with magnetic particles. 300 µl of PBS was added and the sample was suspended (Figure 2.2).

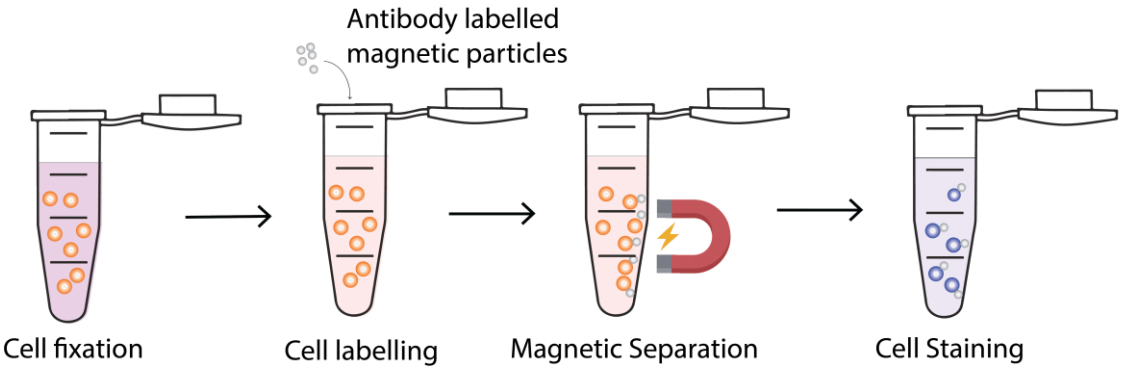

Figure 2.2 Cell preparation.

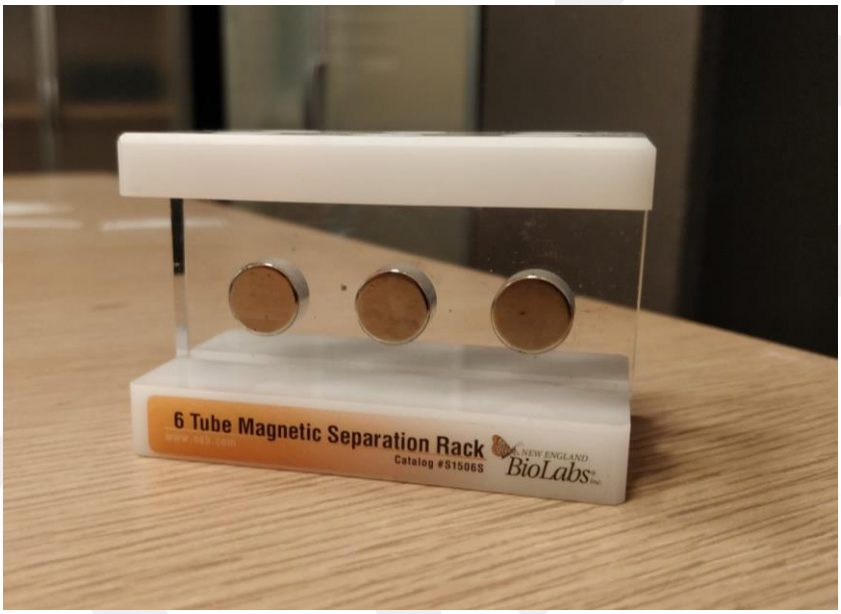

Figure 2.3 Magnetic separation rack

2.4.2 Paper Preparation

In order to get consistent and accurate cut pieces of the sample paper, the sample paper was cut using a laser cutter. The laser cutter used was Epilog Model 10000 30 Watts. The design was created using CorelDRAW. The strips were cut into 5 cm x 0.5 cm strips. The paper was taped on the platform of the cutter and then it was cut. The paper was cut at high speed and low power to avoid burning and blackening of the paper. This method was used for both papers, HF075 and HF135. The cut pieces were then just separated and stored in a box for later use.

2.4.3 Paper-Based Experiment

The cut papers were first wetted using PBS. PBS was added to the paper, and it was left to be absorbed for 10 minutes. After 10 minutes the sample was added in the middle of the paper and a magnetic field was applied using the dual magnet holder. The sample was left in the magnetic field for 10 mins after which the magnetic field was removed, and the control (without the magnetic field) sample and the magnetic field sample were observed under the microscope or taken images of to be processed using the Python code (Figure 2.4).

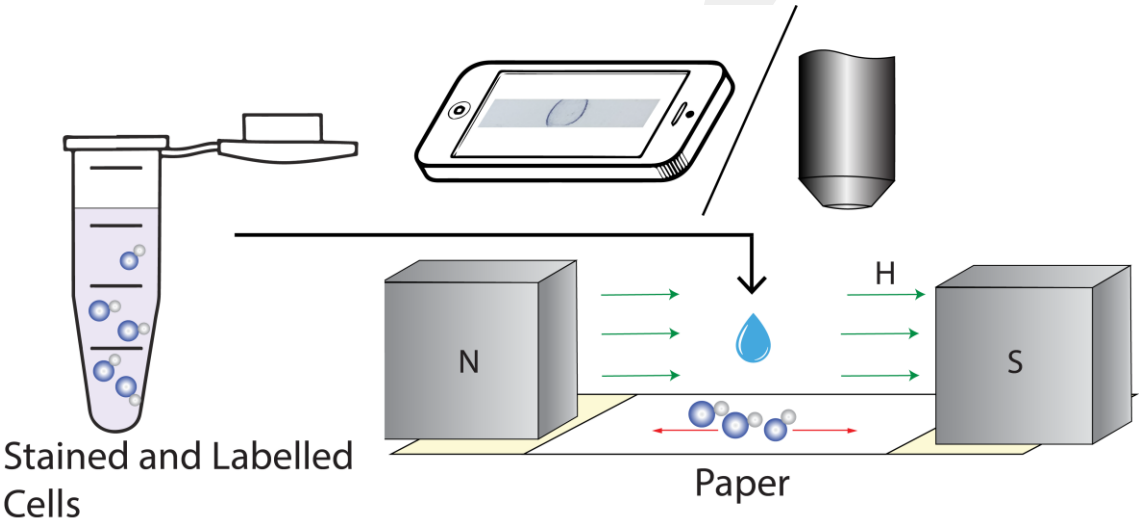

Figure 2.4 The stained and labelled cells were added on the paper after wetting and a magnetic field was applied. Images were then taken using a phone or a microscope.

As shown in Figure 2.5 the magnetic platform allowed the adjustment of the distance between the magnets, thus allowing the manipulation and control of the magnetic field achieved in the middle (Figure 2.5).

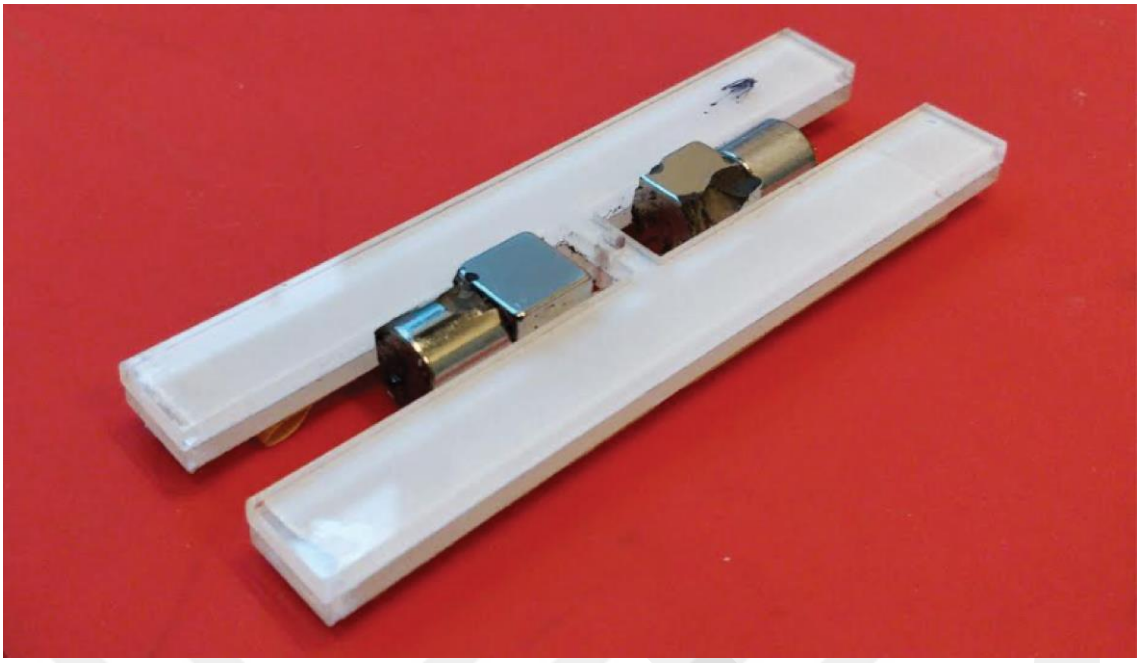

Figure 2.5 The parallel setup of the experiment. Magnetic field was applied parallel to the length of the paper.

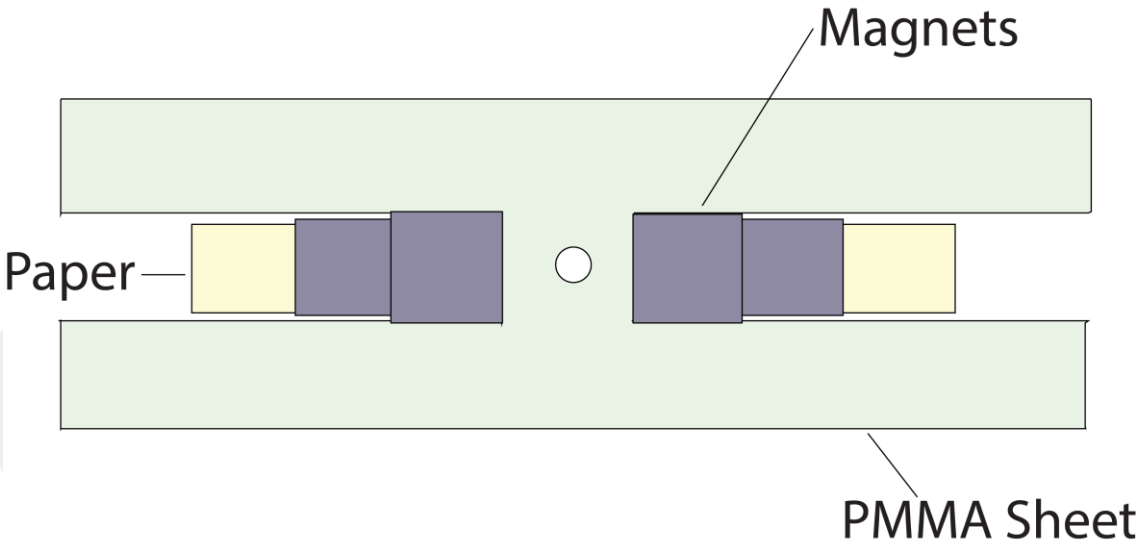

Figure 2.6 The PMMA sheet was used to make the structure, it held the magnets. The magnets were able to be moved so the magnetic field could be varied. Then the experiments could be done with the paper.

2.4.5 BSA Wetting

BSA is Bovine Serum Albumin. It was used to test if the cells would survive for longer on the paper and if it would help with the separation and accumulatio of the sample.

The Paper was made wet using BSA/PBS solution. This solution was created using 10 mg of BSA in 10 ml of PBS which made a 1% BSA in PBS solution. The paper was wetted with 25 µl of BSA/PBS solution and after 10 minutes the sample was added and left for 10 minutes with the magnetic field applied on the sample.

2.4.7 Imaging

The imaging was done using "Nikon Eclipse Ni" and "Nikon Eclipse Ci" at 4x zoom to 50x zoom. "Nikon NIS-Elements" and "ToupView" software were used to take the images. The "Nikon Eclipse Ni" microscope had the Nikon DSRi Camera on it while the "Nikon Eclipse Ci" had the "ToupCam Xcam" had the ToupView camera on it. The sample papers were attached to glass slides and were observed under the microscope.

2.4.8 Magnetic Field Cell Experiments

In this experiment the magnetic field was manipulated and the effect on the movement of the cells was observed. The paper strips were wetted using 25 µl of 1% BSA/PBS solution. The paper was left for 10 mins to absorb the solution after which the sample was introduced in the middle of the paper and the magnetic field was applied across the paper for 10 minutes. After 10 minutes the magnetic field was removed, and the paper was imaged using the microscope and a mobile phone. The magnetic field applied on the paper was varied in this experiment by adjusting the distance between the magnets on the platform and by also using different magnets.

Another set of experiments were also performed in these experiments the HF135 paper was wetted with 30 µl of 1% BSA/PBS after which the labelled cell sample was added and weaker magnetic fields were applied. The time taken for accumulation to be formed at the edge of the paper was measured and the images of the final results were taken and processed.

2.5 Image Processing

Integrating cell phones [43] and image processing [44, 45] with the biosensors was demonstrated in the literature. In this study, the image processing was performed using Python 3. The Python was run on an anaconda environment using visual studio code. The code for image processing was named "PixelAccumulator.py". This code would take the

cropped image of the paper and then it would process the image. The libraries used in this code were, “NumPy”, “Matplotlib”, “SciPy” and “OpenCV”. The code mainly worked using “OpenCV”. OpenCV is a Python library for computer vision applications. The image was read by the code and the pixel values were used to make a quantitative graph. The code would add each Y value at a specific X-axis value, creating a 2D matrix with the X-axis values and the accumulated Y values. From this data a 2D graph was plotted. As shown in Figure 2.7. Since, low pixel value means a darker pixel and a high pixel value means a brighter pixel. Where there were beads or cells present on the paper there were dark spots hence lower pixel values and where there was an absence of beads or cells there were light areas and hence higher pixel values. Hence, the dips in the graphs showed the location of the beads or cells. The code was also scaling the data to 2.5 cm on the x-axis to match it with the length of the paper. As for the y-axis the minimum value of the graph was scaled as 0.

Apart from this the code also found the 2 peaks that were formed by the accumulation of the beads and then reported the distance between the two beads in cm’s. The peaks were found using the SciPy library, to do this the code would first flip the code horizontally and then it would use the “find_peaks” function to find the peaks on the graphs. The code plotted the graph and marked the two peaks on the graph (Figure 2.7).

Since the sample was put in the middle and it was already known that two peaks would be formed during the experimentation, for this reason the code would divide the image into 2 parts vertically (y axis) and then it would find the lowest value in those regions and mark them. The code would then find the distance between the two marked values. This code for most of the images processed and gave the correct results and it was tailored in a way to process images of paper as they had been experimented, meaning the code was specific to a degree and special to the purposes of this research.

The code can be used to process the images with the 3 different channels of the RGB spectrum as well. Red, Green and Blue but for this research this was only done using the total pixel values as in the summation of the values of the 3 channels.

The distance values from the code were taken and plotted. In the case where there was no accumulation of particle as in the case of no magnetic field, the distance value given by the code was not used but instead the focus was put more on the amplitude of the graph and the average of the graph.

The images that were processed were prepared before by cropping to only the region of the sample paper. The code would also mark the detected peaks in the graph it would plot by crosses as it can be seen in Figure 2.7.

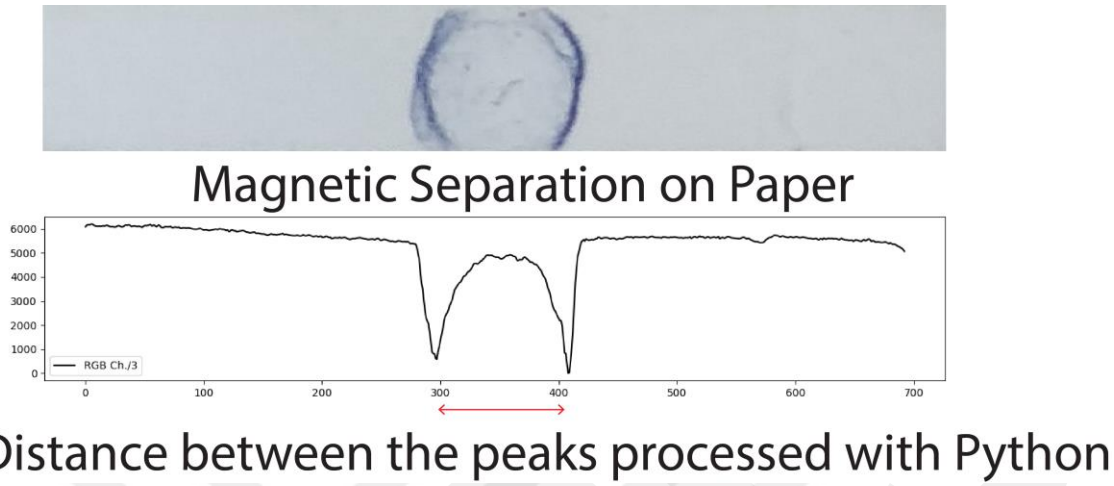

Figure 2.7 The image from the cellphone and the pixel distribution graph.

2.6 COMSOL Simulation

Simulations were performed using COMSOL Multiphysics® 5.4 which is a modeling software. COMSOL is a powerful simulation software and as the name suggests it can create models with different kinds of physics. The models can be made in 2D as well as in 3D while different physics can also be applied to them at the same time. COMSOL has different components that can be added to name a few main ones.

- Electromagnetics Modules
- Fluid Flow & Heat Transfer Modules
- Structural Mechanics & Acoustics Modules
- Chemical Engineering Modules[46]

The setup was designed in the software and then simulations were performed. "Magnetic Fields, No Currents" model was created from the AC/DC module. A 3D model as well as a 2D model was created. The cylinder and cube magnets were designed and simulated in the software.

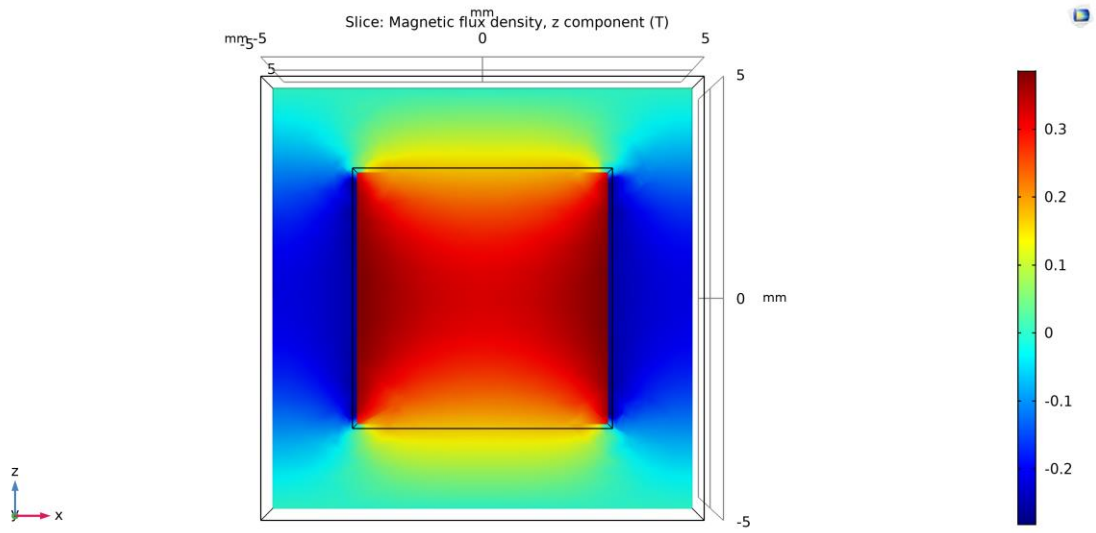

Figure 2.8 Single cube magnet simulation.

First, a single magnet simulation of the cube magnet was made shown in Figure 2.8. The magnet shown in the figure has magnetic flux going into the z direction. The red parts are showing stronger magnetic flux density while the blue parts are showing lower magnetic flux density.

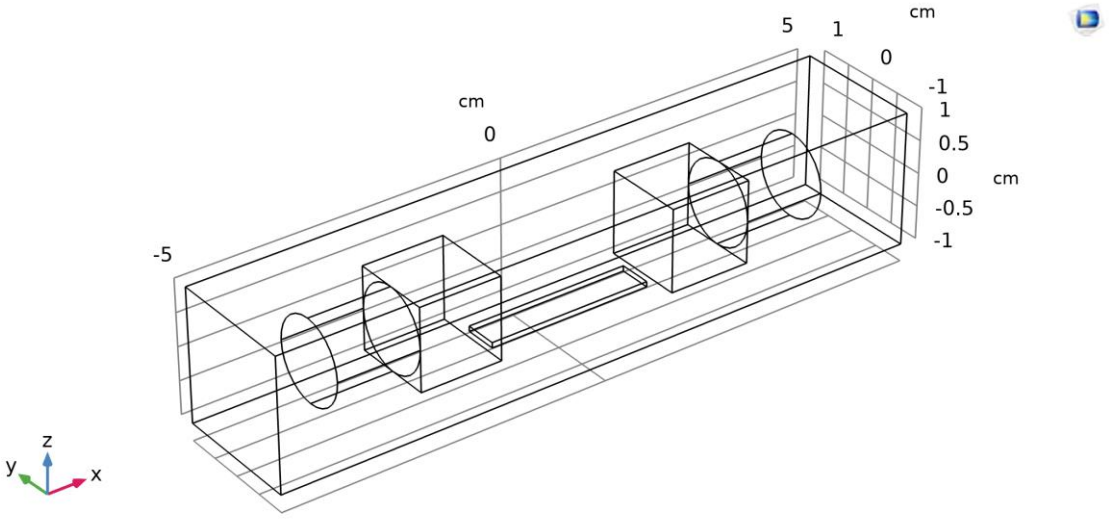

Figure 2.9 The basic model

The basic model is shown in Figure 2.9. For the simulation a cuboid was created around the setup to represent air. The magnetic permeability of air was made to be 1. The 4 magnets were modeled by making domains of magnetic flux conservation. Two of these domains were created for each set of magnets each side producing a magnetic flux in the same directions since the magnets were facing the same direction in the experiments to

create a magnetic field between the magnets. COMSOL allows for different kinds of representations of the simulations.

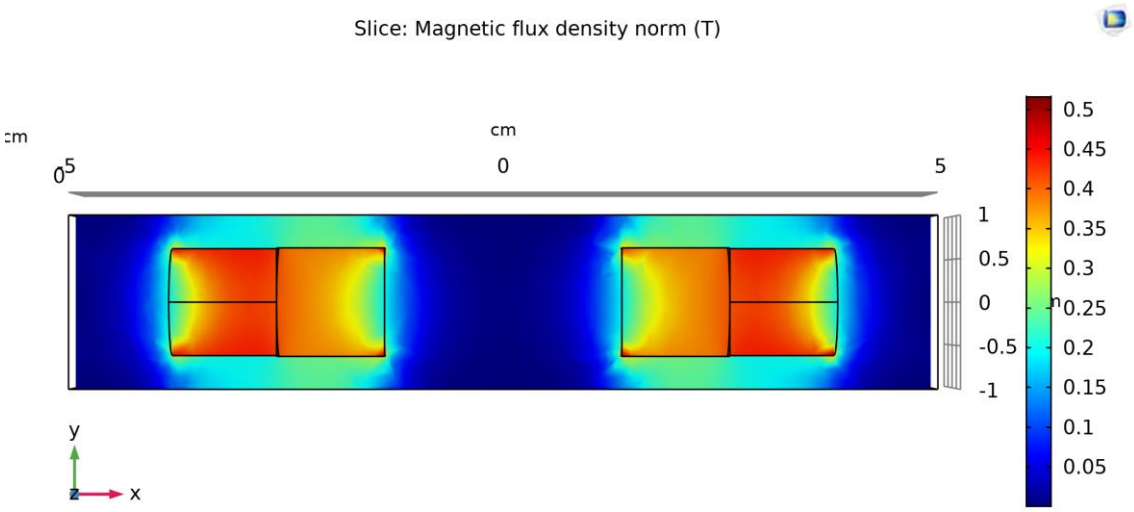

Figure 2.10 Magnetic flux density simulation results. A sliced representation is shown on the plane of z=0.

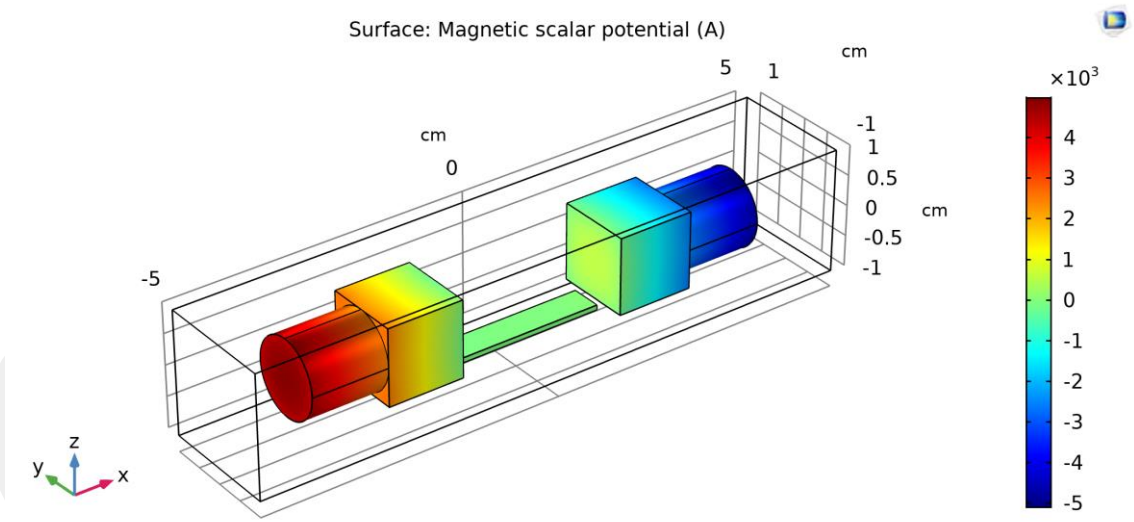

Figure 2.11 This shows the magnetic scalar potential of the setup.

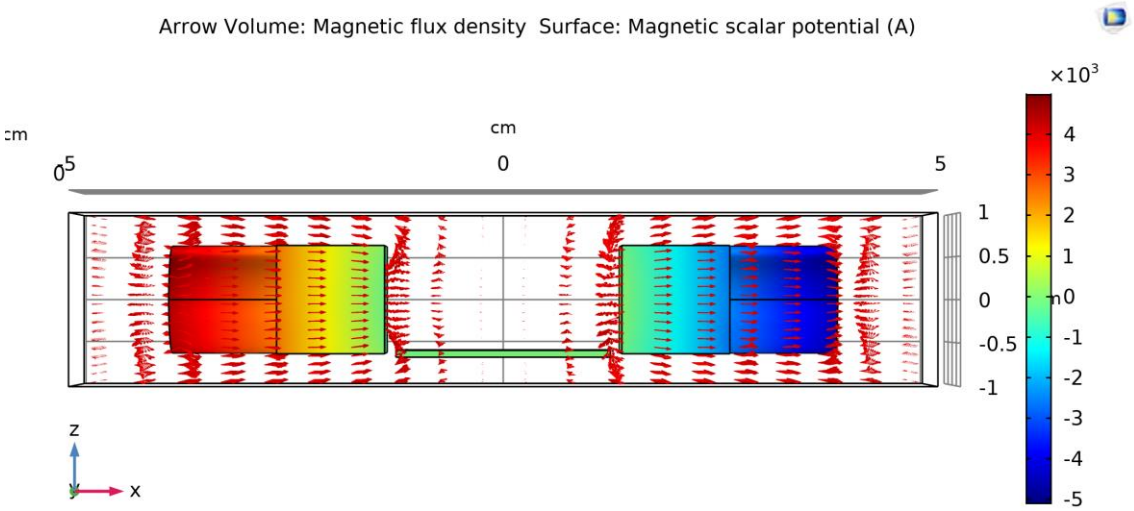

Figure 2.12 Magnetic flux arrow volume.

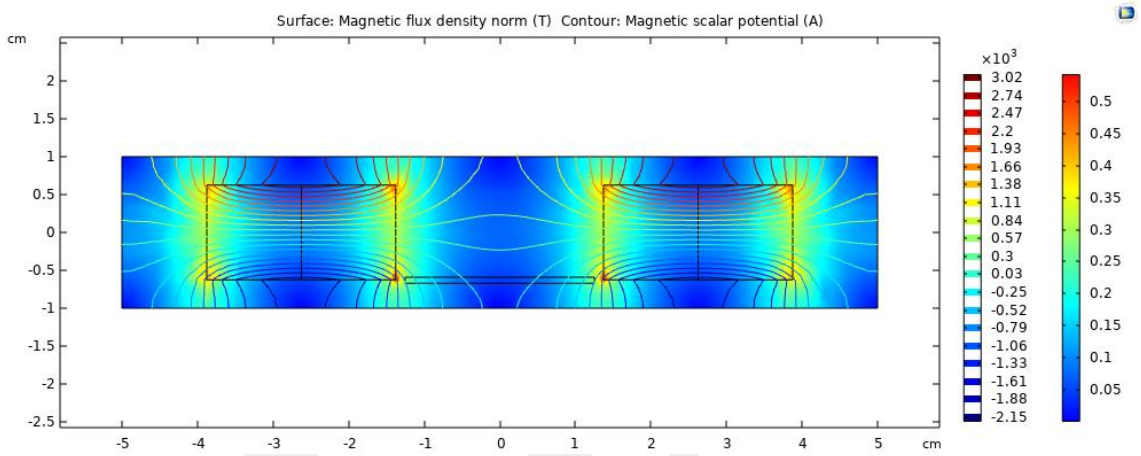

Figure 2.13 2-D Simulation: Magnetic field contour.

The change in magnetic field between the magnet sets was measured and a graph was plotted shown in Figure 2.14. The graph showed similar trends as the experimental results as seen in Figure 3.2.

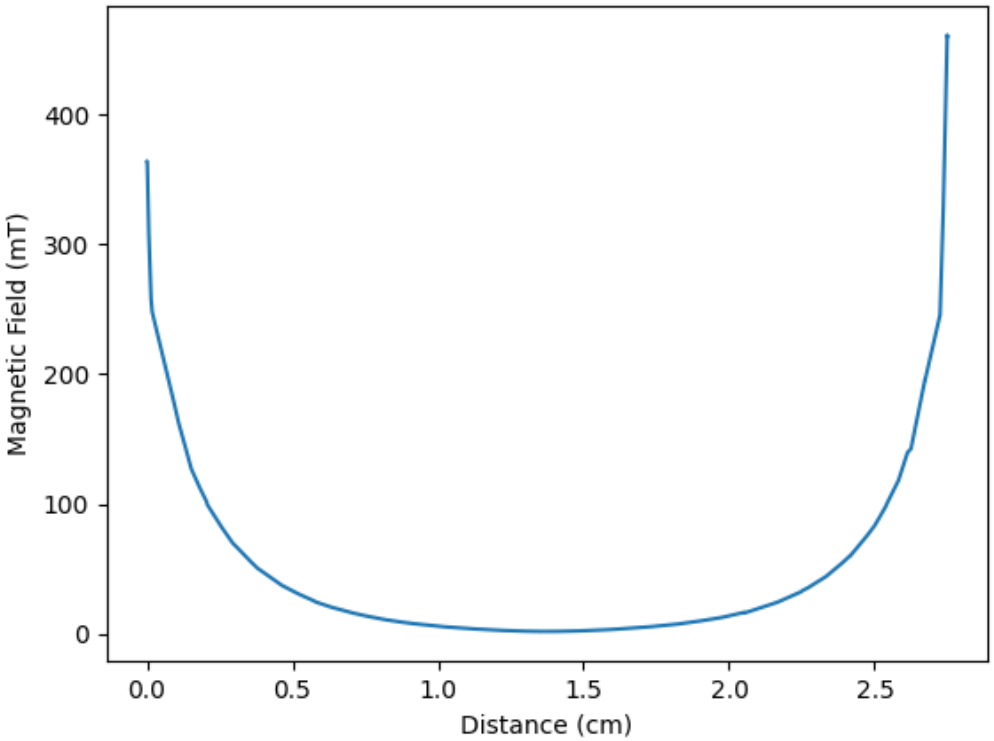

Figure 2.14 Simulation: Change in magnetic field between the magnet sets.

Chapter 3

Results

3.1 Magnetic Force and Wetting

The magnetic field was measured using the gauss meter and the graph was plotted using python. The graph showed that the magnetic field was decreasing exponentially with respect to the distance. Figure 3.1 shows the magnetic field in the middle of the two magnets while the space between the dual magnets is changed. What should be noted in this figure is that in case the measurements were extended to distances less than 2.5 cm, the exponential change would be observed.

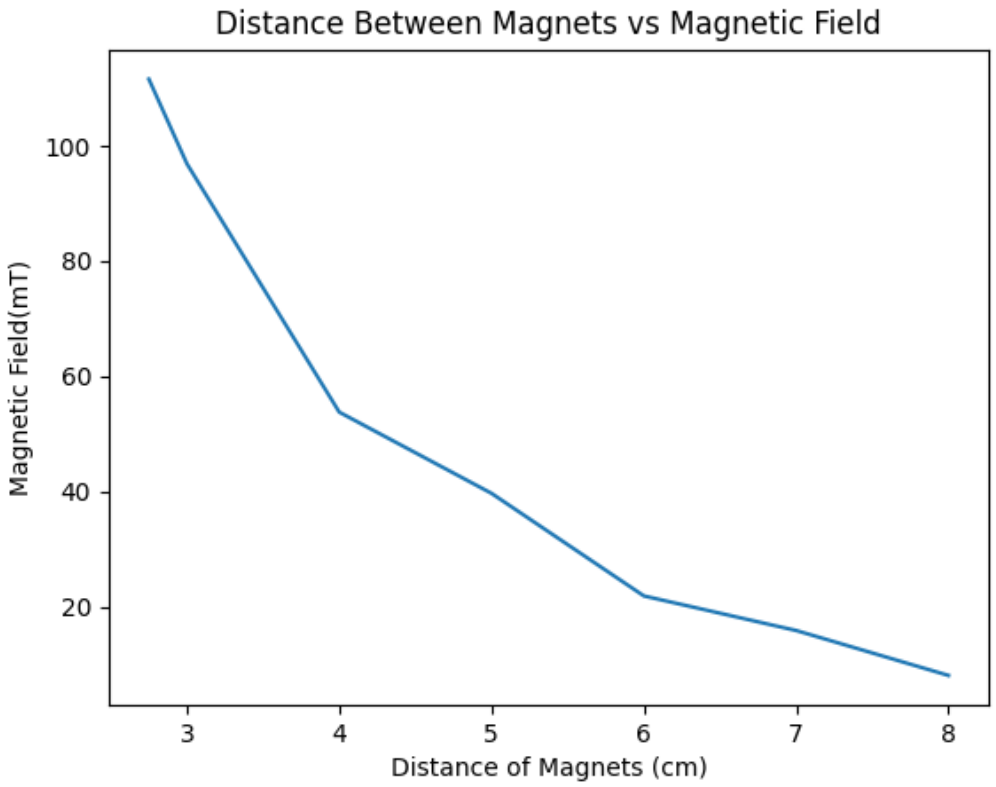

Figure 3.1 The magnetic field in between the dual magnets in respect to position.

The probe of the gauss meter was moved in the space between the two magnets to obtain Figure 3.2 which again led to an exponential double sided curve of sorts.

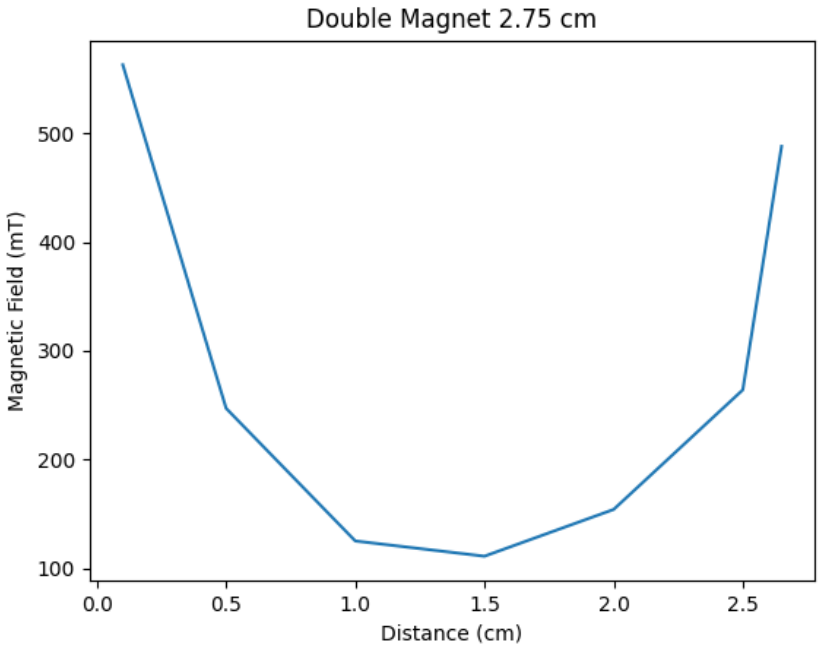

Figure 3.2 The change of magnetic field when the distance between the two magnets is varied from 2.5 cm to 8 cm.

Figure 3.3 shows the effect of the distribution of the particles with respect to the magnetic field applied on the particles. We can see that after the magnetic field becomes weaker than 13.9 mT the accumulation of the particles becomes weak. Since in these experiments the paper was first wetted and then the particles were added directly this caused the particles to quickly reach the edges of the paper, but the effect of the magnetic field can be seen on the density of the accumulation of the particles. The figure also shows graph that shows the distribution and density of the particles as well as the distance between the two accumulation sites. The code also calculated the difference between the average in the middle of the plotted pixel graphs and the amplitude and gave the result. Figure 3.3 shows the sample results and the processing done by the python code. The graph in Figure 3.4 was plotted by using the python code and the distance was calculated similarly.

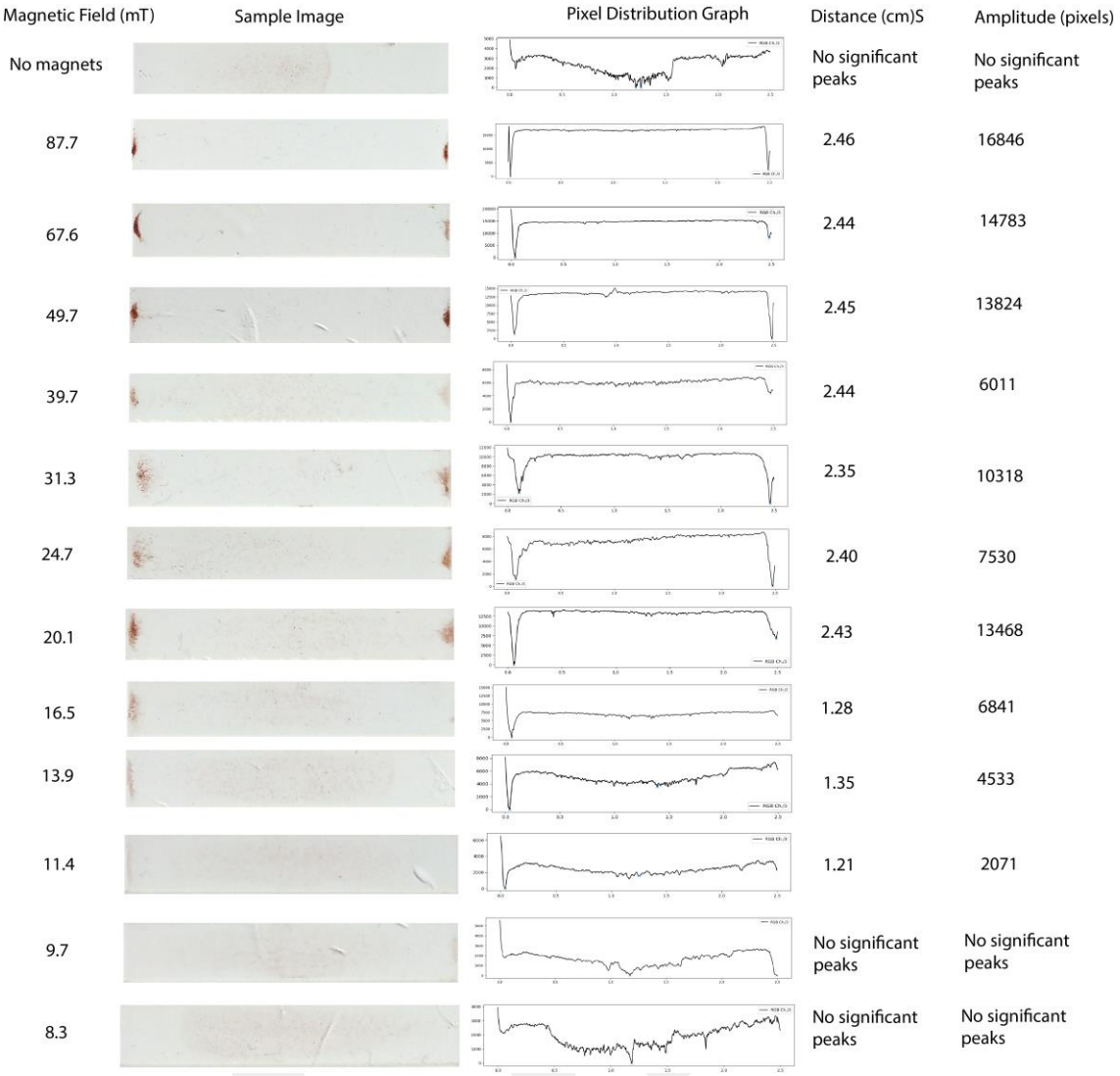

Figure 3.3 Magnetic field experiments and image processing

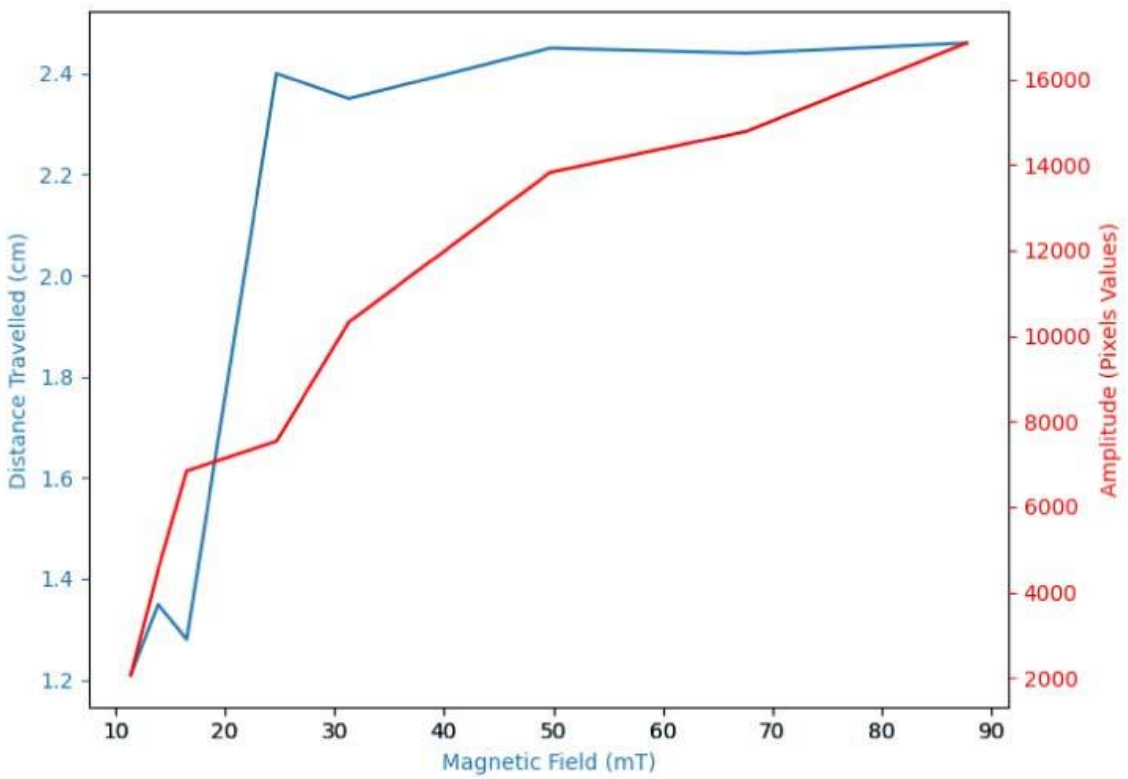

Figure 3.4 The graph of the distance moved by the sample and the amplitude of the graph with respect to the magnetic field, obtained through python

To investigate the effect of wetting on the movement of immunomagnetic particles, different wetting conditions were tested. For this, HF135 paper was used. Increase in wetting resulted in more distance moved by the particles, as well as higher accumulation (Figure 3.5). Initially, in this set up a magnetic field of 244.7 mT was applied using the magnetic platform (1.5 cm) but after 20 µl of wetting the sample began to reach the magnets so the distance was increased to 2.75 cm where the resultant magnetic field was 113.3 mT. Figure 3.4 and Figure 3.5 show the results for both of these conditions.

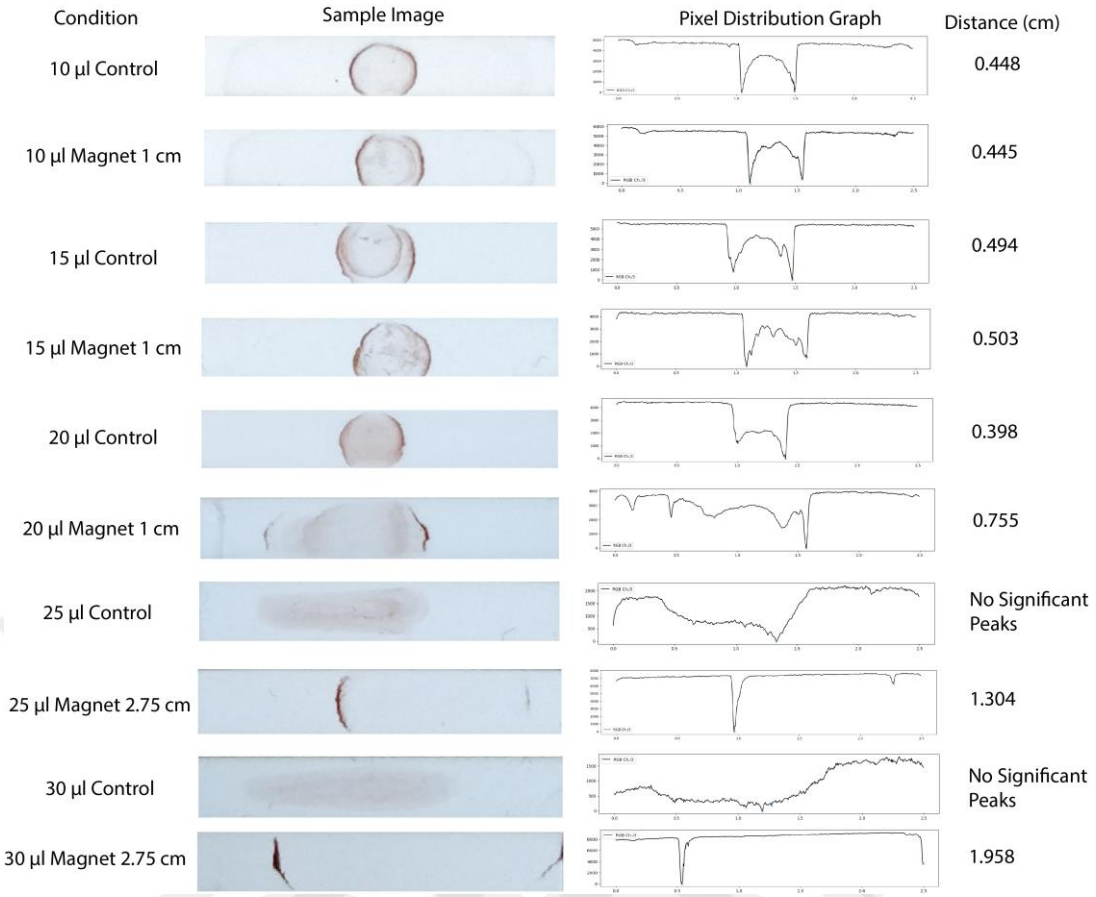

Figure 3.5 The effect of wetting on the separation and accumulation of the immunomagnetic particles.

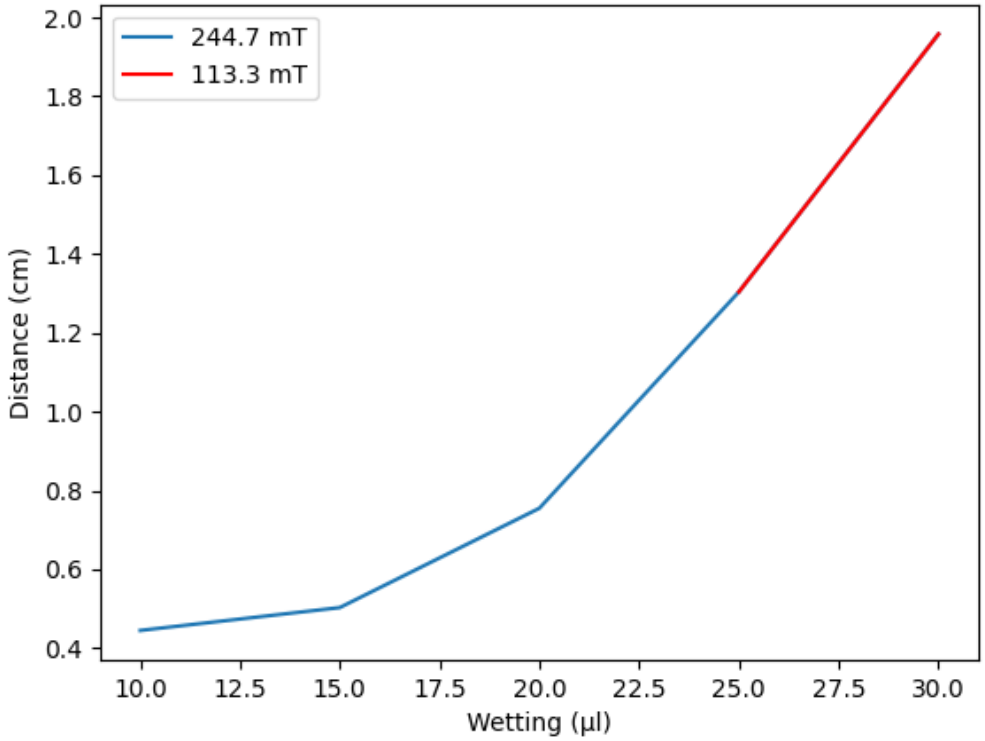

Figure 3.6 Distance moved with respect to wetting in the two magnetic conditions

The HF075 paper has a mean pore size of 14.5 ± 4.7 µm while the HF135 paper has a mean pore size of 11.6 ± 4.06 µm. In comparisons done on the two paper it was found that HF075 has a higher diffusivity as compared to HF135 [40]. It was also investigated how the distance moved by the sample was affected by the paper. For this, 30 µl of wetting was used while a magnetic field of 110.2 mT was applied. HF075 resulted in the sample travelling more with better separation as compared to HF135 (Figure 3.7).

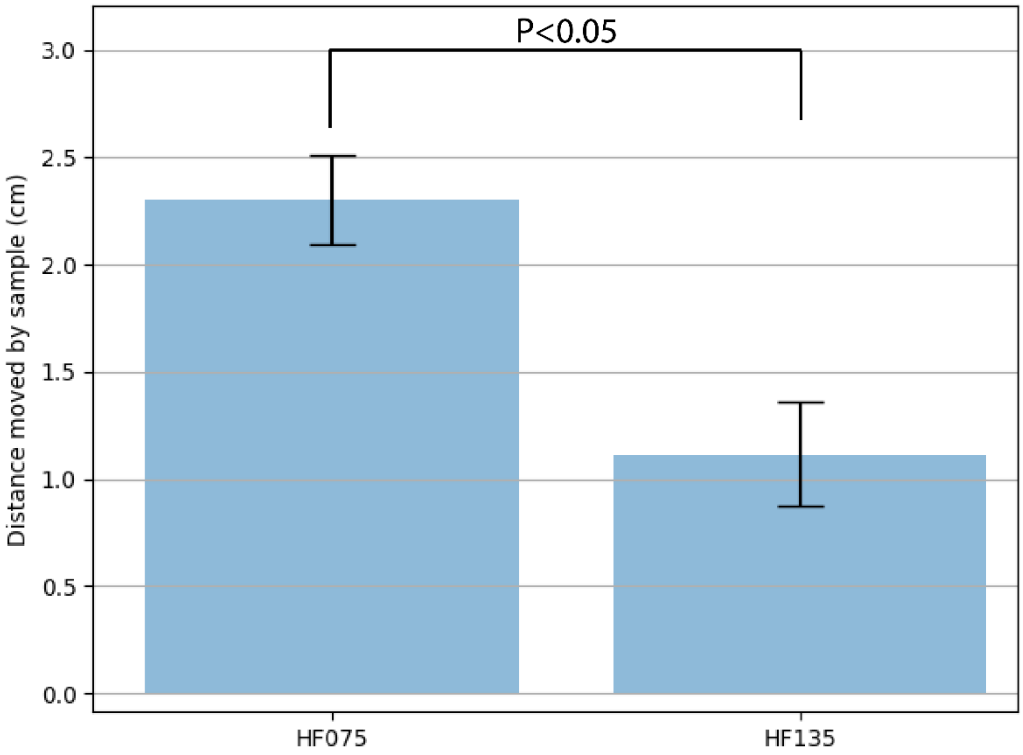

Figure 3.7 Distance moved by the sample on HF075 an HF135 papers

Figure 3.8 and Figure 3.9 show the SEM images of the two papers HF075 and HF135. It can be observed that the HF135 paper is denser as compared to the HF075 paper.

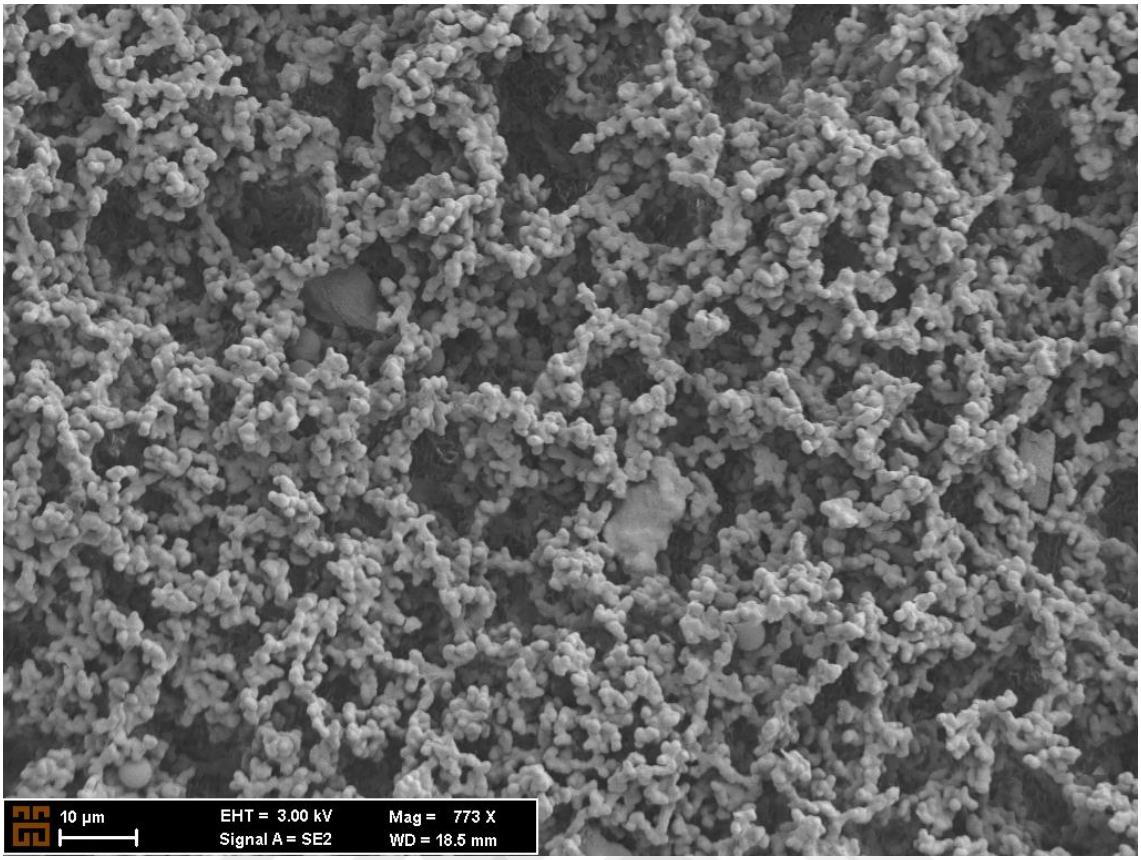

Figure 3.8 SEM image of the HF075 paper

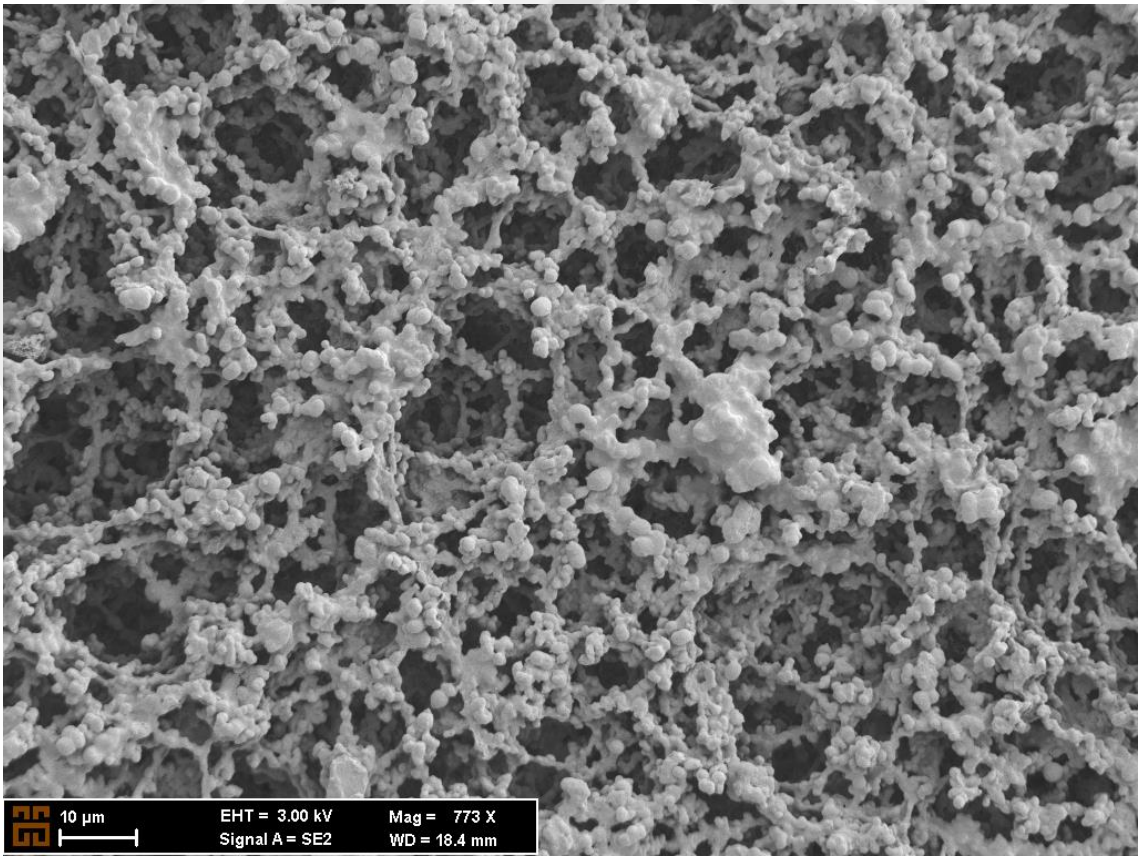

Figure 3.9 SEM image of the HF135 paper

Paper is not the best environment for cells. Since the pores can put the cells in an unfavorable environment causing them to burst. Dryness is one of the factors leading to this as it was seen during the research. The prewetting does not only help with the separating the cells, it also led to the cells surviving for longer on the paper. When no prewetting was applied and the sample was added to the paper the cells would rapidly lose their shape and color. Adding PBS or PBS/BSA as a prewetting increased the cell viability on the paper making them maintain their shape for along. We can see the results for this in Figure 3.10. There were three conditions, no wetting, wetting with PBS and wetting with BSA/PBS. There wasn't statistical significance between the PBS and BSA/PBS conditions but otherwise there was statistical significance in the results.

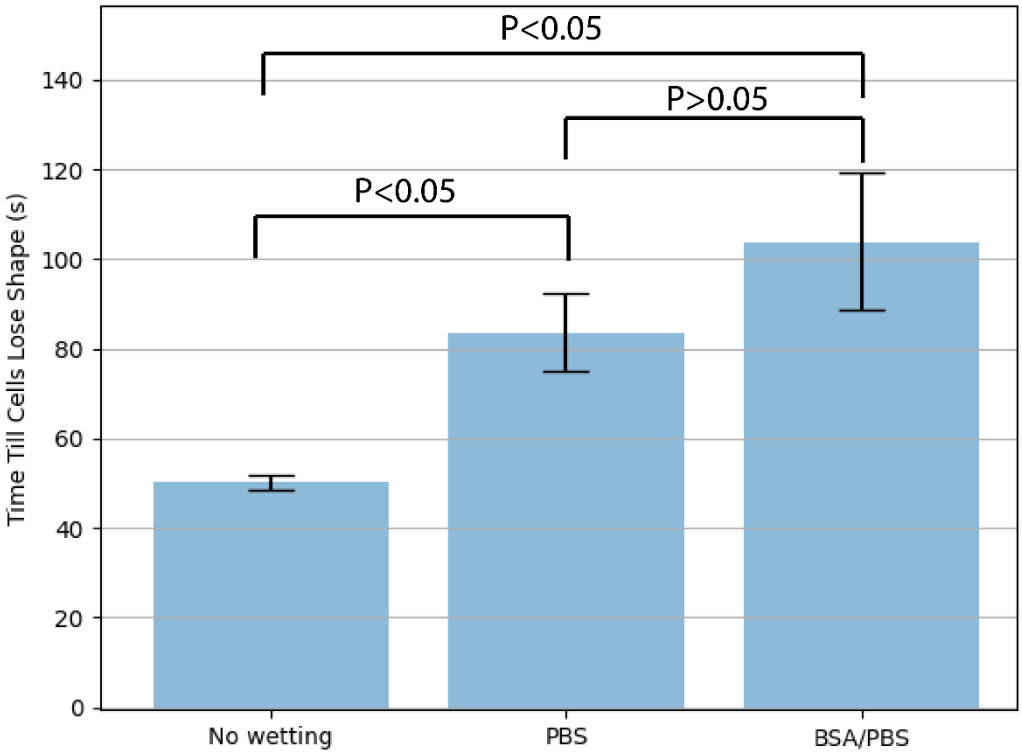

Figure 3.10 The effect of wetting on the cell viability.

3.2 Paper-based Magnetophoresis

The paper was prewetted with 30 µl of BSA/FBS solutions and the magnetic field was manipulated. The travel time of the immunomagnetic beads (along with cells) was recorded. A 5 µl of the sample was added which contained about 2700 cells and it was found that about 90 % of the cells were able to reach the edge of the paper with BSA/BSA wetting.

The increase in magnetic field lead to less time required by the sample to reach the edges of the paper. No significant accumulation was seen after the magnetic field was dropped below 16 mT. 111.6 mT was the highest magnetic field that was applied and it took the least time for the sample to reach the edges at this value (Table 3.1 and Figure 3.11). An exponential decrease was observed in the time taken as the magnetic field was decreased

Magnetic Field/ mT	T_1 (s)	T_2 (s)	T_3 (s)	T_{avg} (s)
111.6	3	3	3	3.00
96.9	4	3	3	3.33
53.8	7	7	6	6.67
39.7	15	17	10	14.0
21.9	25	26	20	23.7
15.9	146	90	57	97.7

Table 3.1 The results from the cells and magnetic field experiments. There were three repeats. T_{avg} is the average of the time taken for the sample to reach the edges.

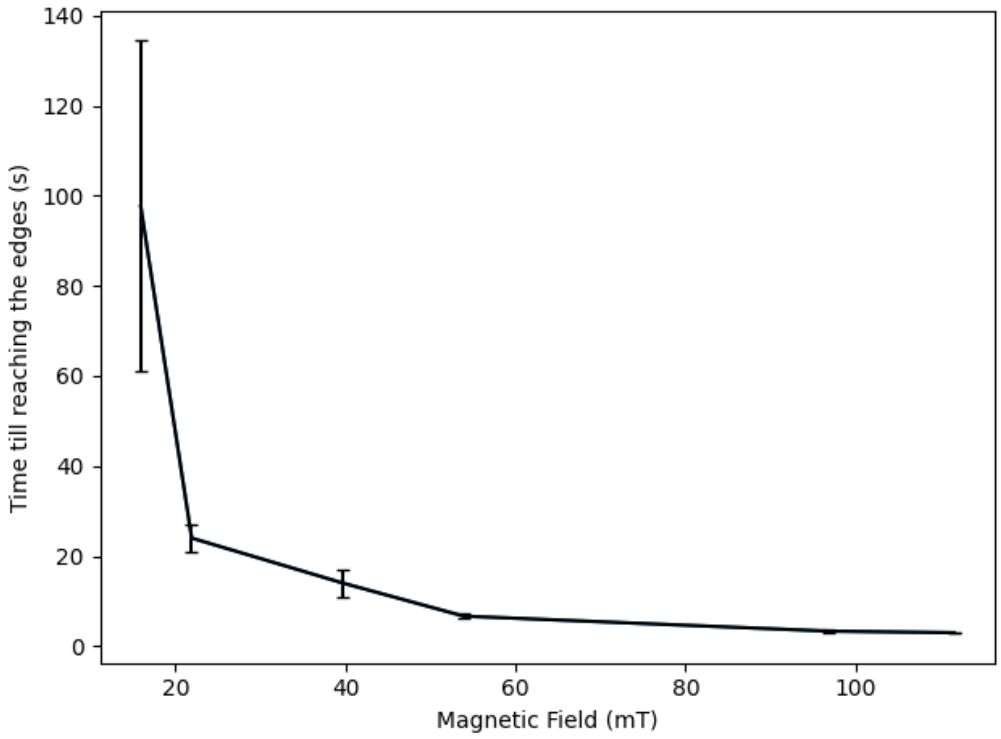

Figure 3.11 The time taken for the sample to reach the edges with respect to the magnetic field.

The blue spots on the paper are the cells while the red spheres are the immunomagnetic particles (Figure 3.12). The magnetic field would make the sample move and make accumulations as we can see in Figure 3.13.

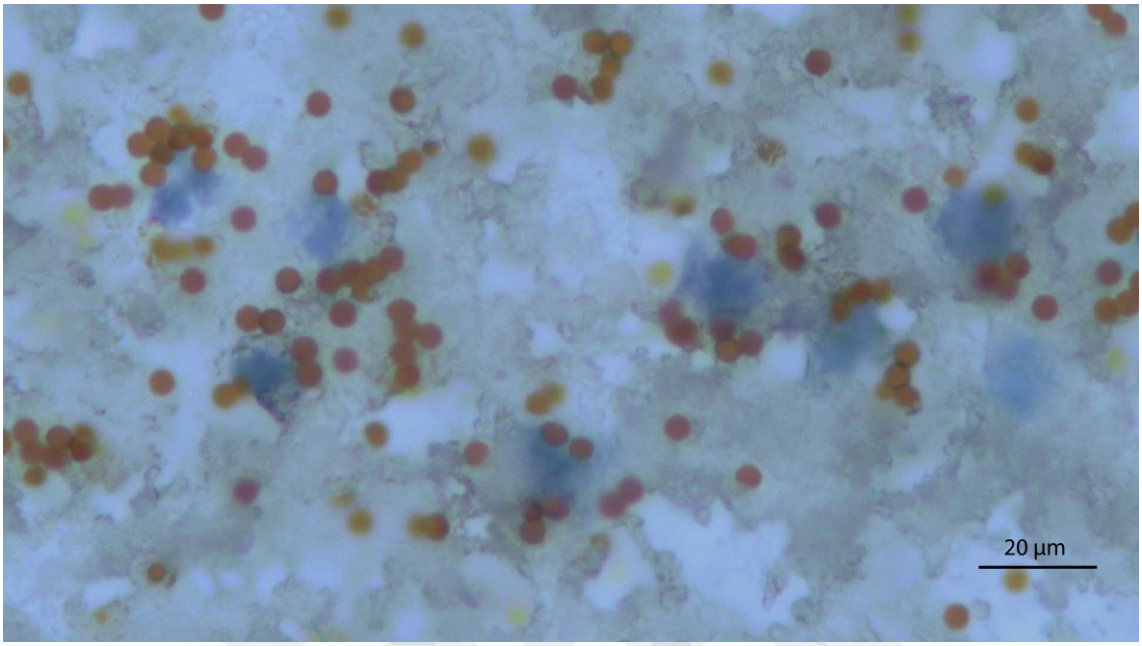

Figure 3.12 The labelled and stained cell sample at 50x in the control condition (no magnetic field).

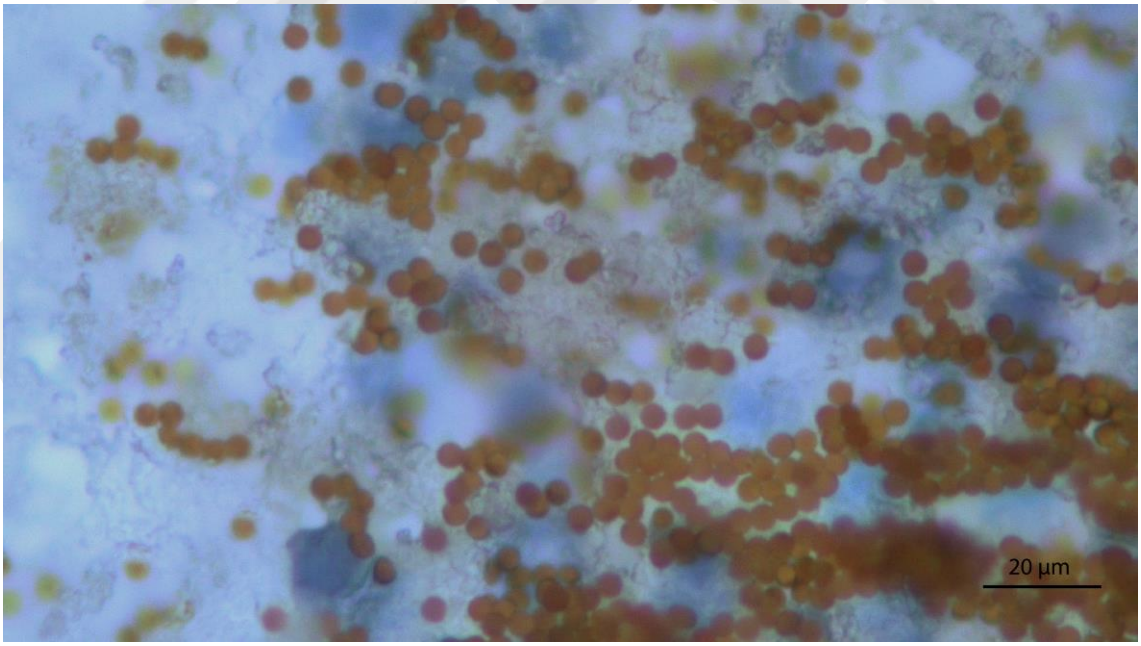

Figure 3.13 The labelled and stained cell sample on paper at 50x in the magnetic condition.

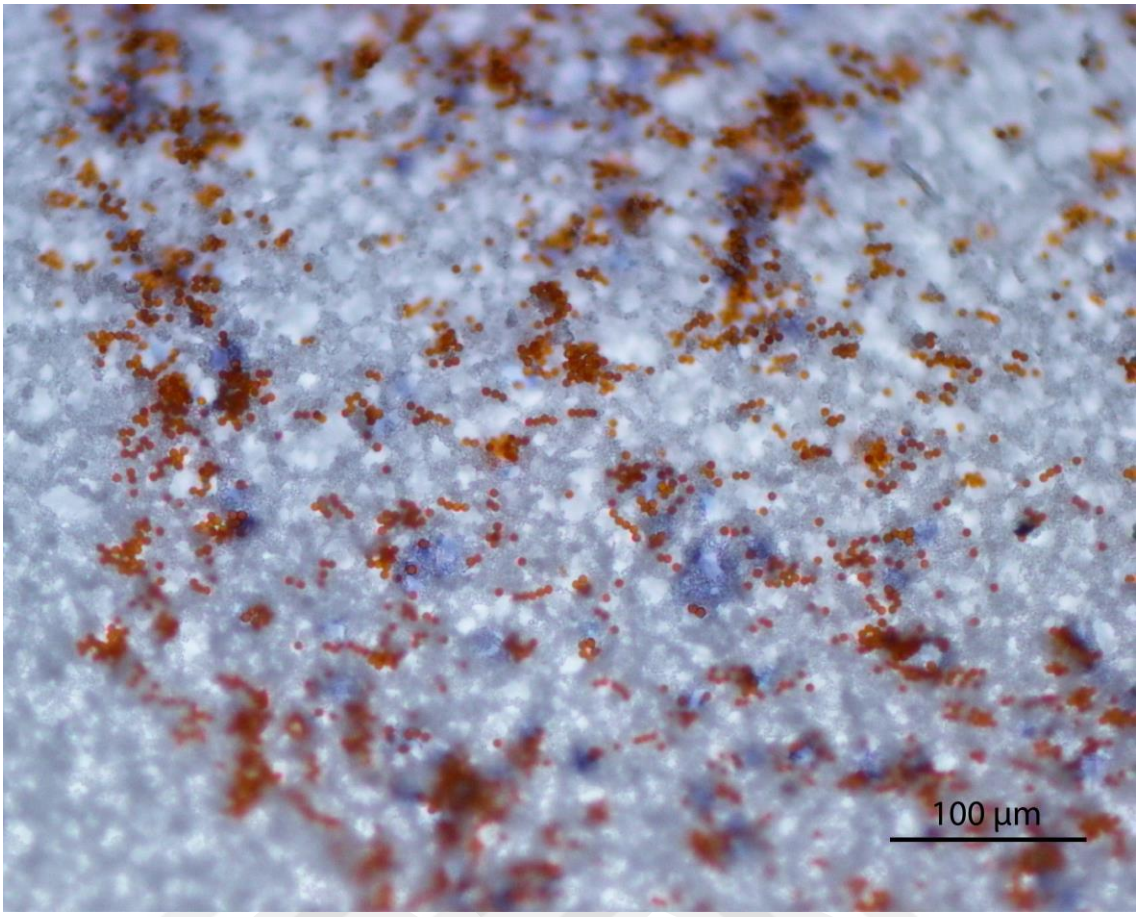

Figure 3.14 The labelled and stained cell sample at 20x in the control condition

The cells are visible on the paper as blue spots but did not maintain their shape because the paper is not the ideal environment for the cells. The red-brown spheres are the immunomagnetic beads (Figure 3.12). Not all of them labelled the cells but if a lower number of IMBs were used the cells would not get labelled properly. Looking at the SEM images we can see that the cells were breaking apart and taking up a flat pancake like shape. Figure 3.15 and Figure 3.16 show the SEM images of the cells and magnetic particles on the paper.

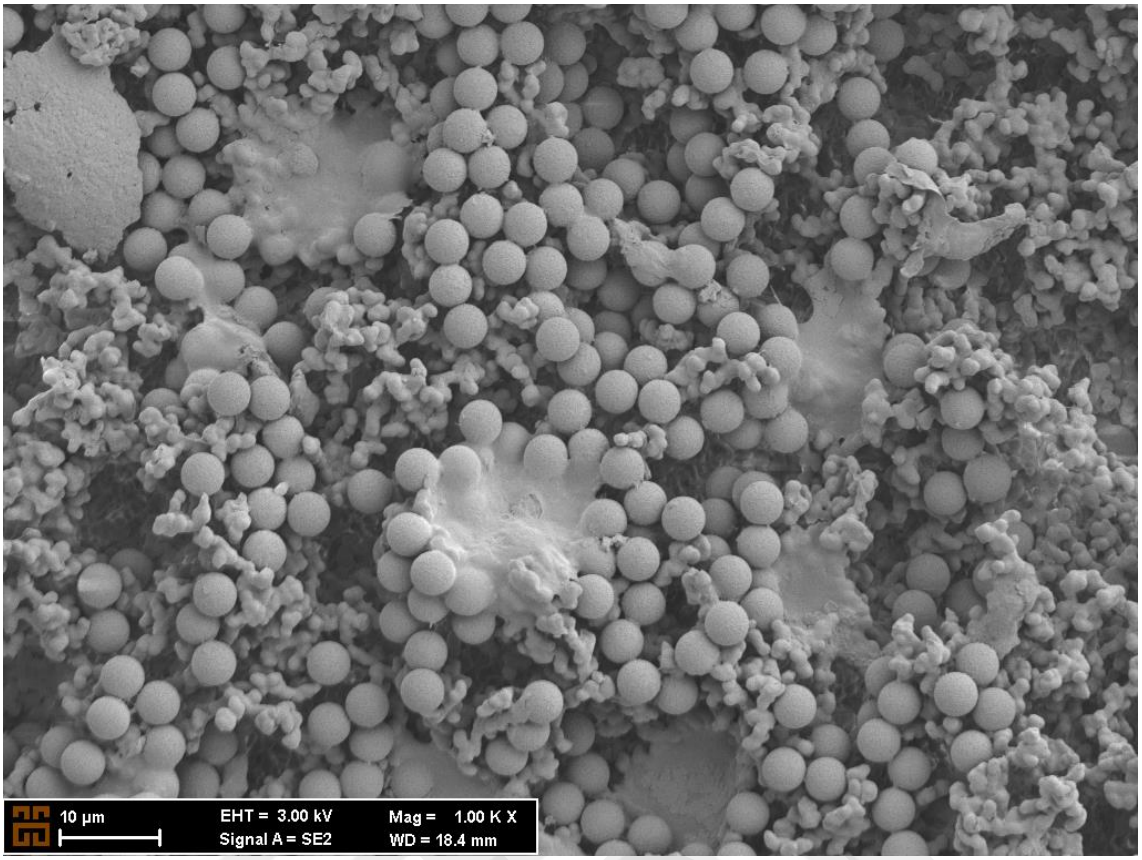

Figure 3.15 Cells and the immunomagnetic particles on the HF075 paper

Figure 3.17 shows the SEM image of the experiment where just a cell sample without the magnetic particles was experimented with. We can see the popped and flattened cells on the surface of the paper. Figure 1.3 shows just the immunomagnetic particles on the HF075 paper. In the labelled cell experiments the sample would accumulate; this accumulation would include the immunomagnetic particles and the cells labeled with the immunomagnetic cells. The accumulation of this sample on the paper can be seen in Figure 3.18

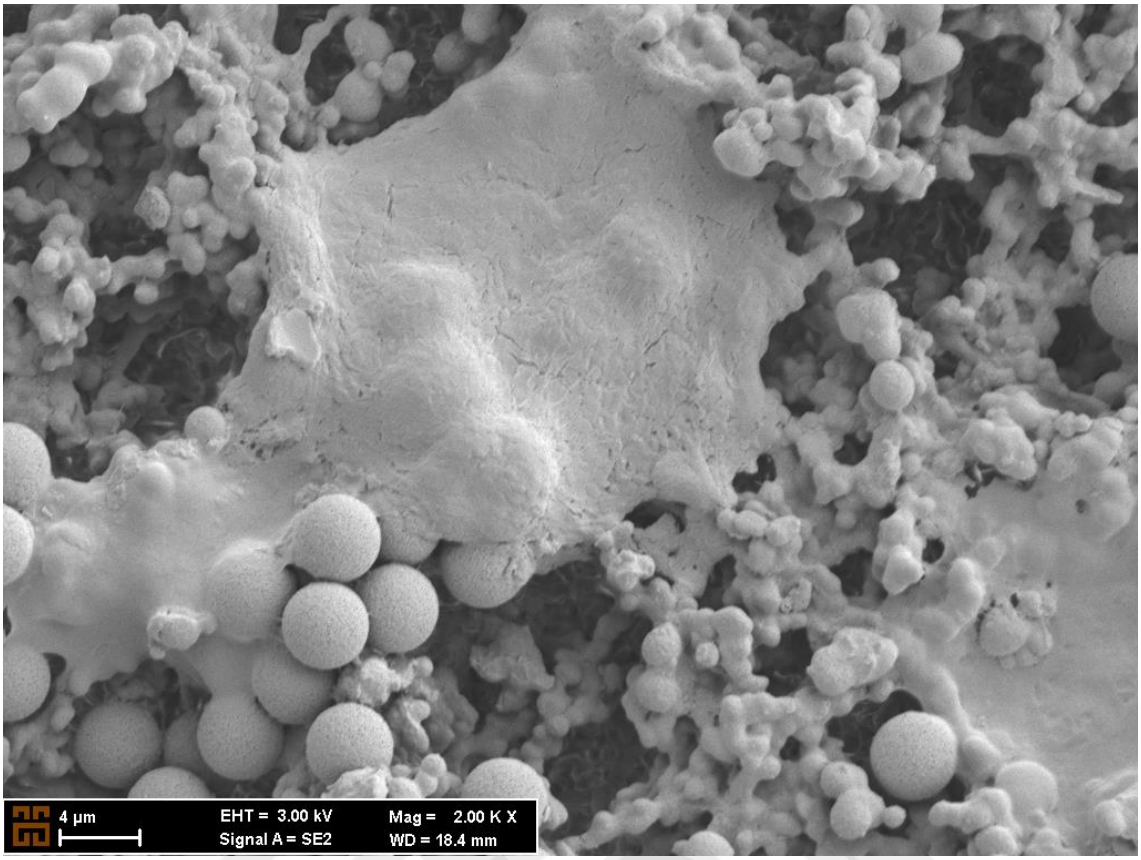

Figure 3.16 Cells and immunomagnetic particles on the HF135 paper

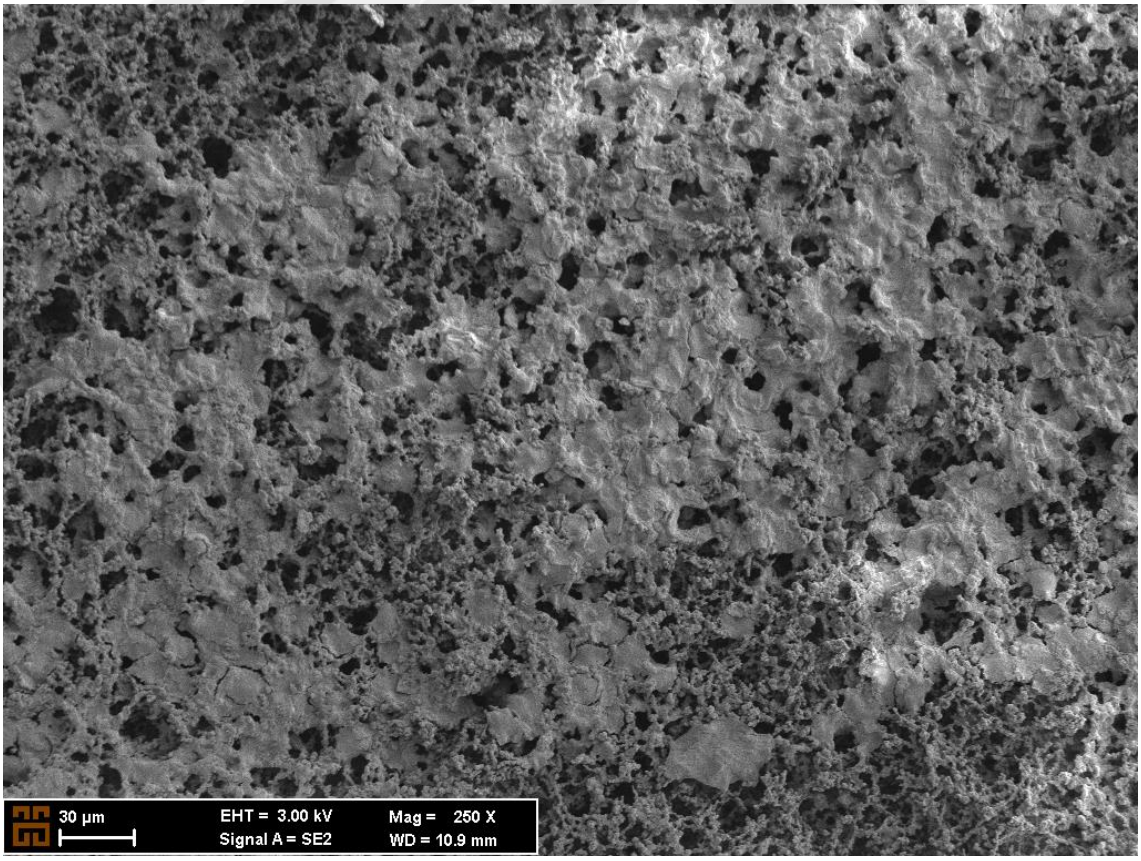

Figure 3.17 K562 cells on the HF135 paper

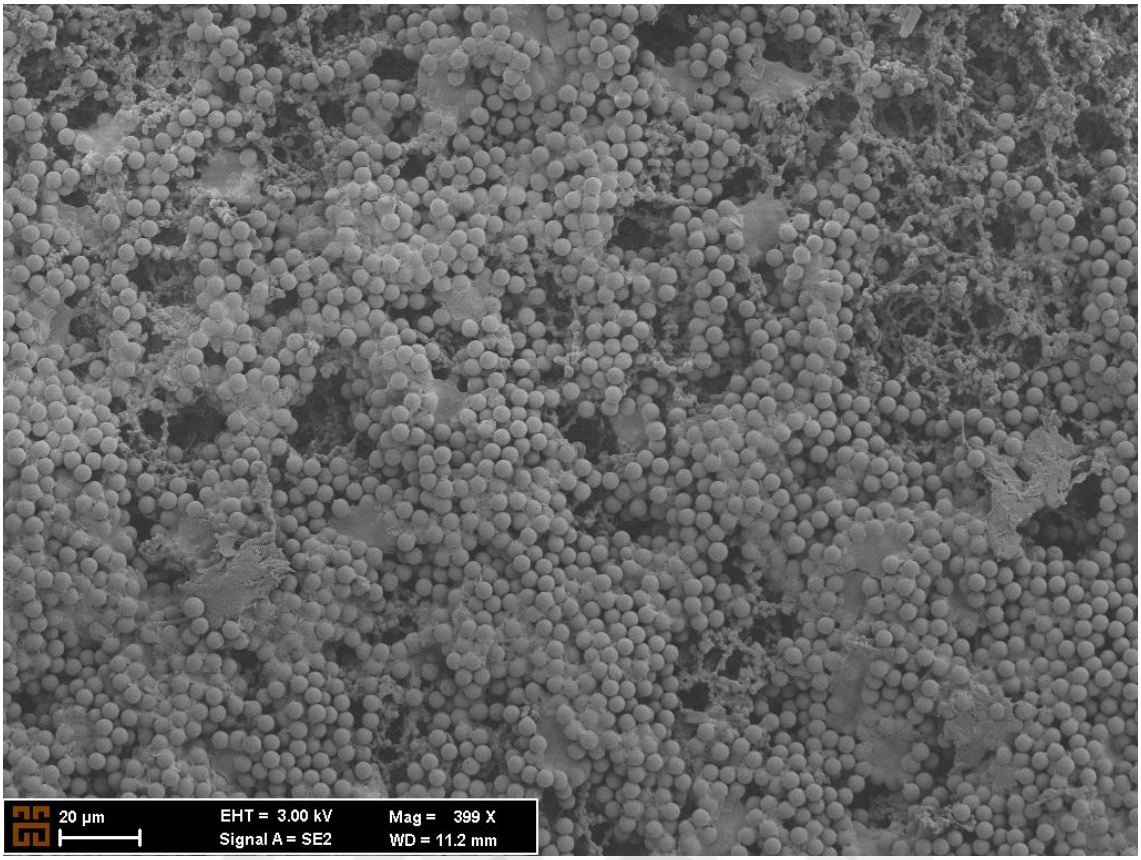

Figure 3.18 Accumulated cells and immunomagnetic particles on the HF135 paper.

Chapter 4

Discussion and Conclusion

4.1 Discussion

The paper used in this research is made of nitrocellulose and it not quite ideal for the cells. This is because it has pores which lead the cell to break open. Also, it applied a force on the delicate cell walls of the cells. That being said, paper-based sensors can lead to cheaper and faster sensing. In this research an external magnetic field was applied, and the cells labelled by magnetic particles were manipulated. The sample would move on the paper and the basic factors that governed this were the magnetic field applied and the wetting applied. The sample was made to travel about 1.25 cm on the paper from the center to the edges and this was done by applying sufficient amounts of wetting and the magnetic field. By using theoretical and experimental data, calculations were made and it was found that the permanent magnets were inducing about 98.5 pN of force on the magnetic particles. The python code was able to process the images making graphs that allowed the understanding of the distribution of the sample on the paper. Along with that it was also able to calculate distance between the peaks that were formed by the sample on the paper.

As mentioned earlier, wetting was an important factor which was affecting the separation of the sample on the paper. Wetting would allow the sample to move on the paper. At lower wetting the sample was not able to move well on the paper. At the same time the wetting also allowed for a suitable environment for the cells to survive on the paper for a bit longer before the cells ended up bursting due to the osmotic imbalance. In the experiments it was seen that cells in the wetted condition were able to survive for longer, compared to non-wetted condition Also compared to non-wetted condition the cells were able to survive for a comparably longer time in the BSA/PBS solution. Even thought, the cells were fixed they were not able to maintain their shape for too long, this

is probably because the paper is not an ideal environment for the cells resulting to plasmolysis. The wetting led to the cells surviving longer on the paper but as the paper dried off the cells would break.

The performance of the paper would be affected by the temperature and this would sometimes lead to different results. Thus the room temperature of the lab could affect the behavior of the paper. [47]

The manufacturer has stated in their datasheet that the difference between the two papers, HF075 and HF135 was that their flowrates and pore sizes were different. HF135 had a slower flow rate compared to HF075. Through the experiments it was seen that flow rate of HF075 paper was faster, but the absorption rate of liquid was slower, compared to HF135. The reason for this might be because HF135 had a higher porosity thus it allows more of the liquid to be absorbed providing a less wetted platform for the sample leading the sample to move less.

The magnetic field would affect the amount of force that was applied on the sample. The wetting would allow the sample to move but the magnetic force was what made the sample move. In the experiment with the labelled cells, where the magnetic field was varied, the time taken for the sample to reach the edges would decrease as the applied magnetic field was increased. This decrease in time was exponential. The cells were moving on the wetted paper's surface through the wetting liquid in dry/non-wetted conditions the cells were not able to move.

The fluid transport in paper can be modelled using Darcy's law, an analogy with an electrical circuit can be made. The pressure difference created can be taken as a voltage source and the volumetric flow rate cane be taken as the current [48]. The magnetic field can be modelled as a secondary voltage source which is in series to the existing voltage source in the model. This secondary source further increases the flow rate of the sample.

The experiments showed that at least 90% of the cells reached the edges of the paper while the rest of the cells were stuck in the middle of the paper. This problem could be solved by using an even stronger magnetic field which would apply a stronger force on the sample leading to more movement of the sample. It was also observed that a small number of the cells were not labelled by magnetic particles and hence did not move because of the magnetic field.

4.2 Societal Impact and Contribution to Global Sustainability

This research has shown that a paper-based biosensing device can be created to be used with cells. This can help to create devices to be used for different kinds of disease detection and even separation of cells. Similar to LFAs these sensors would be easier to use as it was discussed earlier in the thesis. Likewise, since these sensors are based on paper systems, they are cheaper as well. This means that sensors like these can be used in remote areas where there is limited access to lab equipment or facilities [6]. A cheap and easy to use sensor would be helpful for the whole society, in case of disease outbreaks, rapid and affordable testing would help in curbing the spread of disease. From this research it can also be seen that getting results from this system was not time consuming and thus a fast response system would be beneficial.

Since this system is paper based it means that it is a sustainable sensor, this is due to the fact that paper is easy to recycle. Magnetophoretic sensors are usually made using materials like plastic or polydimethylsiloxane and others. Compared to these materials paper is easier to recycle and thus it is easier to take care of the waste produced by these sensors. This kind of sensor can be economically sustainable as well. Since paper-based sensors are cheaper, as discussed earlier.

Such sensors would not only benefit in having a positive impact on the society but at the same time it would benefit by helping promote global sustainability. If further research is continued on such sensors and they are improved to have them accessible by the public and by the health organizations, it could have a beneficial impact on not just the society but the environment as well. If further progress is made these sensors can be ideal for use in healthcare.

4.3 Conclusion and Future Prospects

As mentioned earlier paper-based sensors present the ideal characteristics of a biosensor, high sensitivity, low cost, to mention a few. These qualities along with the specificity and efficiency of the immunomagnetic particles can create an ideal biosensor, one which can specifically separate or detect a target cell or even certain microorganisms like bacteria. Immunomagnetic particles allow us to specifically target a specific antigen by the help of the antigens on the immunomagnetic particles. In order to effectively

perform separation, it must be ensured that the cell that have to be separated are the only ones that are expressing the antigen that the immunomagnetic beads would bind with. Thus, it should be noted that it should be first notified that which antigen is only expressed by the target cell and this can be challenging.

There is not much research done paper-based magnetophoretic biosensors for cells, in this research it was proven that this topic has a promising future. Paper-based magnetophoretic biosensors are cheap and easier to use compared to other kinds of biosensors. Through this research the important parameters and the behavior of the paper was understood. Further research can be done by specifically separating a specific cell from a cell sample with multiple cells. Thus, a quick and cheap sensing device can be created as a cheap, and quick point of care method.

BIBLIOGRAPHY

[1] N. Bhalla, P. Jolly, N. Formisano, and P. Estrela, "Introduction to biosensors," *Essays Biochem.*, vol. 60, no. 1, p. 1, Jun. 2016, doi: 10.1042/EBC20150001.

[2] B.-D. Chan, K. Icoz, W. Huang, C.-L. Chang, and C. A. Savran, "On-demand weighing of single dry biological particles over a 5-order-of-magnitude dynamic range," *Lab Chip*, vol. 14, no. 21, 2014, doi: 10.1039/c4lc00765d.

[3] B. Da Chan, F. Mateen, C. L. Chang, K. Icoz, and C. A. Savran, "A compact manually actuated micromanipulator," *J. Microelectromechanical Syst.*, vol. 21, no. 1, pp. 7–9, 2012.

[4] B.-D. Chan, K. Icoz, R. L. Gieseck, and C. A. Savran, "Selective weighing of individual microparticles using a hybrid micromanipulator-nanomechanical resonator system," *IEEE Sens. J.*, vol. 13, no. 8, 2013, doi: 10.1109/JSEN.2013.2262269.

[5] S. Vigneshvar, C. C. Sudhakumari, B. Senthilkumaran, and H. Prakash, "Recent advances in biosensor technology for potential applications - an overview," *Front. Bioeng. Biotechnol.*, vol. 4, no. FEB, p. 11, Feb. 2016, doi: 10.3389/FBIOE.2016.00011/BIBTEX.

[6] R. Ung *et al.*, "Point-of-Care Screening for Sickle Cell Disease By a Mobile Micro-Electrophoresis Platform," *undefined*, vol. 126, no. 23, pp. 3379–3379, Dec. 2015, doi: 10.1182/BLOOD.V126.23.3379.3379.

[7] P. B. Luppa, C. Müller, A. Schlichtiger, and H. Schlebusch, "Point-of-care testing (POCT): Current techniques and future perspectives," *TrAC Trends Anal. Chem.*, vol. 30, no. 6, pp. 887–898, Jun. 2011, doi: 10.1016/J.TRAC.2011.01.019.

[8] K. İçöz *et al.*, "Immunomagnetic separation of B type acute lymphoblastic leukemia cells from bone marrow with flow cytometry validation and microfluidic chip measurements," *https://doi.org/10.1080/01496395.2020.1835983*, vol. 56, no. 15, pp. 2659–2666, 2020, doi: 10.1080/01496395.2020.1835983.

[9] K. İçöz, T. Gerçek, A. Murat, S. Özcan, and E. Ünal, "Capturing B type acute lymphoblastic leukemia cells using two types of antibodies," *Biotechnol. Prog.*, vol. 35, no. 1, p. e2737, Jan. 2019, doi: 10.1002/btpr.2737.

[10] K. Icoz, M. C. Soylu, Z. Canikara, and E. Unal, "Quartz-crystal Microbalance Measurements of CD19 Antibody Immobilization on Gold Surface and Capturing

B Lymphoblast Cells: Effect of Surface Functionalization," *Electroanalysis*, vol. 30, no. 5, pp. 834–841, May 2018, doi: 10.1002/ELAN.201700789.

[11] K. İçöz, Ü. Akar, and E. Ünal, "Microfluidic Chip based direct triple antibody immunoassay for monitoring patient comparative response to leukemia treatment," *Biomed. Microdevices*, vol. 22, no. 3, p. 48, Sep. 2020, doi: 10.1007/s10544-020-00503-6.

[12] A. Munaz, M. J. A. Shiddiky, and N. T. Nguyen, "Recent advances and current challenges in magnetophoresis based micro magnetofluidics," *Biomicrofluidics*, vol. 12, no. 3, May 2018, doi: 10.1063/1.5035388.

[13] Y. Y. Huang *et al.*, "Screening and Molecular Analysis of Single Circulating Tumor Cells Using Micromagnet Array," *Sci. Rep.*, vol. 5, no. 1, p. 16047, Nov. 2015, doi: 10.1038/srep16047.

[14] O. Osman *et al.*, "Microfluidic immunomagnetic cell separation using integrated permanent micromagnets," *Biomicrofluidics*, vol. 7, no. 5, Sep. 2013, doi: 10.1063/1.4825395.

[15] J. Darabi and C. Guo, "Continuous isolation of monocytes using a magnetophoretic-based microfluidic Chip," *Biomed. Microdevices*, vol. 18, no. 5, Oct. 2016, doi: 10.1007/s10544-016-0105-8.

[16] N. Xia *et al.*, "Combined microfluidic-micromagnetic separation of living cells in continuous flow," *Biomed. Microdevices*, vol. 8, no. 4, pp. 299–308, Dec. 2006, doi: 10.1007/s10544-006-0033-0.

[17] J. Pivetal *et al.*, "Micro-magnet arrays for specific single bacterial cell positioning," *J. Magn. Magn. Mater.*, vol. 380, pp. 72–77, Apr. 2015, doi: 10.1016/J.JMMM.2014.09.068.

[18] D. Quesada-González and A. Merkoçi, "Nanoparticle-based lateral flow biosensors," *Biosensors and Bioelectronics*, vol. 73. Elsevier Ltd, pp. 47–63, Nov. 05, 2015, doi: 10.1016/j.bios.2015.05.050.

[19] C. Parolo *et al.*, "Tutorial: design and fabrication of nanoparticle-based lateral-flow immunoassays," *Nat. Protoc. 2020 1512*, vol. 15, no. 12, pp. 3788–3816, 2020, doi: 10.1038/s41596-020-0357-x.

[20] R. H. Shyu, H. F. Shyu, H. W. Liu, and S. S. Tang, "Colloidal gold-based immunochromatographic assay for detection of ricin," *Toxicon*, vol. 40, no. 3, pp. 255–258, Mar. 2002, doi: 10.1016/S0041-0101(01)00193-3.

[21] D. Mazumdar, J. Liu, G. Lu, J. Zhou, and Y. Lu, "Easy-to-use dipstick tests for

detection of lead in paints using non-cross-linked gold nanoparticle-DNAzyme conjugates," *Chem. Commun.*, vol. 46, no. 9, pp. 1416–1418, Feb. 2010, doi: 10.1039/b917772h.

[22] S. F. Torabi and Y. Lu, "Small-molecule diagnostics based on functional DNA nanotechnology: A dipstick test for mercury," *Faraday Discuss.*, vol. 149, pp. 125–135, 2011, doi: 10.1039/c005404f.

[23] X. Wang *et al.*, "Development of an immunochromatographic lateral-flow test strip for rapid detection of sulfonamides in eggs and chicken muscles," *J. Agric. Food Chem.*, vol. 55, no. 6, pp. 2072–2078, Mar. 2007, doi: 10.1021/jf062523h.

[24] H. Leem, S. Shukla, X. Song, S. Heu, and M. Kim, "An Efficient Liposome-Based Immunochromatographic Strip Assay for the Sensitive Detection of SalmonellaTyphimurium in Pure Culture," *J. Food Saf.*, vol. 34, no. 3, pp. 239–248, Aug. 2014, doi: 10.1111/jfs.12119.

[25] P. Zhou *et al.*, "Nanocolloidal gold-based immunoassay for the detection of the N-methylcarbamate pesticide carbofuran," *J. Agric. Food Chem.*, vol. 52, no. 14, pp. 4355–4359, Jul. 2004, doi: 10.1021/jf0499121.

[26] K. Inoue, P. Ferrante, Y. Hirano, T. Yasukawa, H. Shiku, and T. Matsue, "A competitive immunochromatographic assay for testosterone based on electrochemical detection," *Talanta*, vol. 73, no. 5, pp. 886–892, Oct. 2007, doi: 10.1016/j.talanta.2007.05.008.

[27] M. J. Jacinto *et al.*, "Enhancement of lateral flow assay performance by electromagnetic relocation of reporter particles," *PLoS One*, vol. 13, no. 1, p. e0186782, Jan. 2018, doi: 10.1371/JOURNAL.PONE.0186782.

[28] I. M. Hsing, Y. Xu, and W. Zhao, "Micro- and nano- magnetic particles for applications in biosensing," *Electroanalysis*, vol. 19, no. 7–8. pp. 755–768, Apr. 2007, doi: 10.1002/elan.200603785.

[29] A. G. Kolhatkar, A. C. Jamison, D. Litvinov, R. C. Willson, and T. R. Lee, "Tuning the magnetic properties of nanoparticles," *International Journal of Molecular Sciences*, vol. 14, no. 8. pp. 15977–16009, 2013, doi: 10.3390/ijms140815977.

[30] K. Icoz, B. D. Iverson, and C. Savran, "Noise analysis and sensitivity enhancement in immunomagnetic nanomechanical biosensors," *Appl. Phys. Lett.*, vol. 93, no. 10, 2008.

[31] O. Mzava, Z. Tas, and K. İçöz, "Magnetic micro/nanoparticle flocculation-based signal amplification for biosensing," *Int. J. Nanomedicine*, vol. 11, pp. 2619–2631,

2016, doi: 10.2147/IJN.S108692.

[32] K. İçöz and O. Mzava, "Detection of Proteins Using Nano Magnetic Particle Accumulation-Based Signal Amplification," *Appl. Sci.*, vol. 6, no. 12, p. 394, Nov. 2016, doi: 10.3390/app6120394.

[33] C. Y. Huang *et al.*, "Magnetic micro/nano structures for biological manipulation," *SPIN*, vol. 6, no. 1, 2016, doi: 10.1142/S2010324716500053.

[34] G. Karp, *Cell biology.*, Seventh. Wiley, pp. 720-725, 2014.

[35] B. J. Graham, "Antibody." https://www.genome.gov/genetics-glossary/Antibody (accessed Dec. 17, 2021).

[36] M. Hejazian, W. Li, and N. T. Nguyen, "Lab on a chip for continuous-flow magnetic cell separation," *Lab on a Chip*, vol. 15, no. 4. Royal Society of Chemistry, pp. 959–970, Feb. 21, 2015, doi: 10.1039/c4lc01422g.

[37] N. T. Nguyen, "Micro-magnetofluidics: Interactions between magnetism and fluid flow on the microscale," *Microfluid. Nanofluidics*, vol. 12, pp. 1–16, 2012, doi: 10.1007/s10404-011-0903-5.

[38] G. Ablay, M. Böyük, and K. İçöz, "Design, modeling, and control of a horizontal magnetic micromanipulator," *Trans. Inst. Meas. Control*, vol. 41, no. 11, pp. 3190–1398, 2019, doi: 10.1177/0142331218824392.

[39] E. W. Washburn, "The dynamics of capillary flow," *Phys. Rev.*, vol. 17, no. 3, p. 273, 1921, doi: 10.1103/PhysRev.17.273.

[40] H. Li and B. Eng, "Qualitative Blood Coagulation Test Using Paper-Based Microfluidic Lateral Flow Device." 2014.

[41] G. Ablay, M. Böyük, Y. Eroğlu, and K. İçöz, "A horizontal magnetic tweezer for single molecule micromanipulations," 2018, p. 6, doi: 10.1109/ISMSIT.2018.8567067.

[42] K. Icoz and C. Savran, "Nanomechanical biosensing with immunomagnetic separation," *Appl. Phys. Lett.*, vol. 97, no. 12, p. 123701, 2010.

[43] K. Içöz, "Image processing and cell phone microscopy to analyze the immunomagnetic beads on micro-contact printed gratings," *Appl. Sci.*, vol. 6, no. 10, 2016, doi: 10.3390/app6100279.

[44] F. Uslu, K. Icoz, K. Tasdemir, R. S. Doğan, and B. Yilmaz, "Image-analysis based readout method for biochip: Automated quantification of immunomagnetic beads, micropads and patient leukemia cell," *Micron*, vol. 133, p. 102863, 2020, doi: 10.1016/j.micron.2020.102863.

[45] F. Uslu, K. Icoz, K. Tasdemir, and B. Yilmaz, “Automated quantification of immunomagnetic beads and leukemia cells from optical microscope images,” *Biomed. Signal Process. Control*, vol. 49, pp. 473–482, Mar. 2019, doi: 10.1016/J.BSPC.2019.01.002.

[46] “The COMSOL® Software Product Suite.” https://www.comsol.com/products (accessed Dec. 18, 2021).

[47] N. Walji and B. D. MacDonald, “Influence of Geometry and Surrounding Conditions on Fluid Flow in Paper-Based Devices,” *Micromachines*, vol. 7, no. 5, 2016, doi: 10.3390/MI7050073.

[48] M. M. Gong and D. Sinton, “Turning the Page: Advancing Paper-Based Microfluidics for Broad Diagnostic Application,” *Chem. Rev.*, vol. 117, no. 12, pp. 8447–8480, 2017, doi: 10.1021/acs.chemrev.7b00024.

APPENDIX

Appendix A: Python Code

```
import cv2
import numpy as np
import matplotlib.pyplot as plt
from scipy.signal import find_peaks

img = cv2.imread('./MT005.jpg')

param = img.shape

print(param)
d=range(0,param[1])
scaleMax = 2.5/param[1]
print (f'scale : {scaleMax}')
d = np.arange(0, 2.5, scaleMax)

ar=[]
ag=[]
ab=[]
a=[]
acc = 0

for i in range(param[1]):
    a.append(0)
    ag.append(0)
    ar.append(0)
    ab.append(0)

for x in range(param[1]):
    count=0
    countb=0
    countg=0
    countr=0
    for y in range(param[0]):
        count = int(img[y,x,0]) + int(img[y,x,1]) + int(img[y,x,2]) + count
        countb = int(img[y,x,0]) + countb
        countg = int(img[y,x,1]) + countg
        countr = int(img[y,x,2]) + countr

    a[x] = count/3
    ab[x] = countb
    ag[x] = countg
    ar[x] = countr

print (f'type: {type(d)} | size: {len(d)}') ## X
print (f'type: {type(a)} | size: {len(a)}') ## Y
```

```
min_a = min(a)
new_a = [val - min_a for val in a]

new_a = [a[i] - min_a for i in range(len(a) - 1, -1, -1)]

## inverse horizantal.
new_a_2 = [new_a[i] for i in range(len(new_a) - 1, -1, -1)]
new_a = [val for val in new_a_2]

## DEBUG CHECK | Inverse the graph

plt.plot(d, new_a, color = 'black', label = "RGB Ch./3")

needed_indexes = []
for i, val in enumerate(d):
   if val >= 0.5 and val <= 2.0:
      needed_indexes.append(i)

needed_y_values = []
for idx in needed_indexes:
   needed_y_values.append(new_a[idx])

neededAverage = sum(needed_y_values)/len(needed_y_values)

## Peak 1. First Half
half_1 = [new_a[i] for i in range(0, int(len(new_a)/2))]
inversed_a = [val * -1 for val in half_1]
peak_indexes, _ = find_peaks(inversed_a)

peak_indexes = [val for val in peak_indexes]
peak_values = [half_1[idx] for idx in peak_indexes]

peak_1 = min(peak_values)
idx_1 = peak_indexes[peak_values.index(peak_1)]
idx_1_d = d[idx_1]

## Peak 2. Second Half
half_2 = [new_a[i] for i in range(int(len(new_a)/2), len(new_a))]
inversed_a = [val * -1 for val in half_2]
peak_indexes, _ = find_peaks(inversed_a)

peak_indexes = [val for val in peak_indexes]
peak_values = [half_2[idx] for idx in peak_indexes]

peak_2 = min(peak_values)
idx_2 = peak_indexes[peak_values.index(peak_2)] + int(len(new_a)/2)
idx_2_d = d[idx_2]

print (f'P1: {peak_1} | P2: {peak_2}')
```

```
## Right side override.
if idx_1 < idx_2:
    if peak_2 > new_a[-1]: #d[-1]:
        peak_2 = new_a[-1] #d[-1]
        idx_2 = len(d) - 1
        idx_2_d = d[idx_2]
elif idx_1 > idx_2:
    if peak_1 > new_a[-1]: #d[-1]:
        peak_1 = new_a[-1] #d[-1]
        idx_1 = len(d) - 1
        idx_1_d = d[idx_1]

## Left side override
if idx_1 > idx_2:
    if peak_2 > new_a[0]: #d[0]:
        peak_2 = new_a[0] #d[0]
        idx_2 = 0
        idx_2_d = d[idx_2]
elif idx_1 < idx_2:
    if peak_1 > new_a[0]:#d[0]: ## 20210512
        peak_1 = new_a[0]#d[0]
        idx_1 = 0
        idx_1_d = d[idx_1]
##
print (f'P1: {peak_1} | P2: {peak_2}')

print (f'div : {int(len(new_a)/2)}')
print (f'actual : {int(len(new_a))}')
print (f'peak values {peak_1}, {peak_2}')
print (f'peak idxs {idx_1}, {idx_2}')

peaks_ = np.asarray([idx_1, idx_2])
peaks_d = np.asarray([idx_1_d, idx_2_d])
print (f'peaks : {peaks_}')

np_a = np.asarray(new_a)
plt.plot(peaks_d, np_a[peaks_], "x")

d_1 = d[peaks_[0]]
d_2 = d[peaks_[1]]
difference_result = abs(d_1 - d_2)

print(f'test{new_a}')

print (f'Difference between peak positions: {difference_result}')

print (f'Needed Average: {neededAverage}')

plt.legend()
plt.show()
```

CURRICULUM VITAE

2015 – 2019	B.Sc., Eletrical and Electronics Engineering, Abdullah Gul University, Kayseri, TURKEY
2019 – Present	M.Sc., Electrical and Computer Engineering, Abdullah Gul University, Kayseri, TURKEY